Kite aerial photography

A low cost remote sensing tool for ecological research?

- Bart Slot -

ITC

Supervised by:
Prof. dr. J.P. Bakker
Rijksuniversiteit Groningen

Dr. I.C. van Duren
International Institute for Geo-Information Science
and Earth Observation

RuG

D 951

Table of contents

Acknowledgements

This research project couldn't be done without Iris van Duren, Jan Hendriks en Gerard Reinink. Their support was vital for my project. I would like to thank ITC for providing an inspiring work environment and the opportunity to let me be in that environment. I also would like to thank Ton Klomphaar from state forestry service, who allowed me to do my research in their terrain. For guidance and feedback on my writing I thank Professor Jan Bakker.

Abstract

Remote sensing and GIS software is increasingly used in ecological research. Although there is a lot of imagery readily available from different suppliers, the spatial or temporal resolution often don't match the researchers need. Kite aerial photography can be used as a simple low cost remote sensing tool. In this research, kite aerial photographs are taken from a small nature reserve in the east of the Netherlands, 'de Borkeld' (lat,lon: 52.271265°, 6.491023°). The camera used was a normal consumer digital camera (Canon s70).

For use in photogrammetic applications the camera had to be calibrated. The focal length, pixel size on the ccd, principal point and lens distortion were determined using Photomodeler 5. Before the aerial photographs were taken a grid of markers was placed in the study area and their positions and elevation was recorded with a geodetic dGPS. These markers served as ground control points in the georeferencing process. From 16 aerial photographs a mosaic was created covering 16.9 hectares. The mosaic has a ground resolution of 8.7 cm. From a subsection of the mosaic area a highly detailed digital terrain model was constructed.

Using a supervised classification a vegetation map with 5 classes was created. The high resolution of the images gave some problems for the applied classification method. Due to variations in light and shadow, some misclassifications occurred. However the overall result was good. Especially *Molinia caerulea*, a species that replaces the heather vegetation, had a distinct spectral signature and was easy to identify.

The heather coverage mainly consisted of *Calluna vulgaris* with some patches of *Erica tetralix*. By clipping out the heather area from the main image a supervised classification was done using only two classes; *Calluna vulgaris* and *Erica tetralix*. Using this method the patches with *Erica tetralix* could be predicted with high accuracy.

Using kite aerial photography and normal digital cameras for photogrammetic purposes in ecological research shows great potential as a research tool. With the ongoing development of digital camera's and GIS software this method provides a way for researchers to obtain their own aerial images.

Introduction

The use of aerial and satellite images in today's research projects has enormously expanded over the past decade. Spatial data are used in numerous fields such as agriculture, forestry, environment/nature monitoring, disaster assessment, urban development and weather forecasting. And there is a fast amount of data, free accessible on the internet (Aber 2002). However these may not always meet the researchers need. Acquiring spatial data of specific areas at specific moments with specific resolution is very costly and therefore the most significant constraint in the use of spatial data (Baker et al., 2004). A low cost platform capable of acquiring high resolution images would fill up a large gap in aerial remote sensing.

Several researchers have experimented with good results with low flying platforms. Buerkert *et al.* (1996) assessed the technique for monitoring plant growth in the Sahel. Both Gerard *et al.* (1997) and Jia *et al.* (2004) used low aerial photography as a non-destructive method for plant nitrogen status. Stow *et al.* (2004) used a digital camera attached to a small aircraft to map invasions of alien plant species in South African shrub lands. The platforms used in these projects vary from kites, helium balloons to sophisticated remotely controlled helicopters or light aircrafts. Each platform has its own characteristics in terms of stability, ground coverage and experience needed to operate it (Kerle et al., 2005).

The technique of low aerial photography is not new. The first patent issued by the United States Patent Office for a camera system suspended from a kite or balloon was in 1887 by J. Fairman. It is recent technology that causes researchers all over the world to gain interest in this field again. The availability of desktop GIS and high-resolution digital cameras makes the acquisition and geo-referencing of digital imagery significantly simpler.

Low aerial remote sensing is not meant to compete with the conventional satellite and aerial imagery on coverage. The price of a Quickbird image may be high but compared to the covered surface the price paid per square meter is low. Newly acquired georeferenced and orthorectified imagery from the Quickbird satellite (0.6 m. resolution) with the area of interest within the US will cost $63/Km². However the minimum area to buy is 100 km^2 (Satimagingcorp, 17-1-2007) Aerial imagery is more expensive. Nature conservation organizations in the Netherlands usually combine their orders and get the price down to €500/km^2. with a resolution of 15 cm.

Low aerial remote sensing is a solution for small-scale areas.

Kite aerial photography and normal digital cameras for use in photogrammetic applications is a rapidly evolving field. During this project several other researchers explored the possibilities of low aerial remote sensing. The internet proofed again to be a useful medium to exchange information about this subject. This was extremely helpful since there was not much information available in the conventional media.

The possibilities of low aerial remote sensing are fast in potential but are not jet explored in the full extend. An important aspect is that low aerial photography brings the virtues of remote sensing within reach of every researcher who's interested in the spatial relationships of our world.

Research objective and questions

Main objective:
In this research project, a cheap method to acquire high resolution aerial images, will be developed and tested. The obtained images are used to create a high resolution geo-rectified map and a digital elevation model (DEM). These will be used for terrain analysis.

Specific objectives:

- To asses the suitability of a kite as an aerial camera platform
- To produce geo-rectified images with a consumer digital camera
- To create highly detailed maps with the composition and structure of heath land vegetation.

Research hypothesis
Normal digital cameras can be used to take very high resolution aerial images on any given platform. The images can be precisely geo-rectified and mosaiced to serve a base map. The image data can be analysed and used in ecological research.

Research questions:

- Is it possible to calibrate a non-metric consumer digital camera to be used for cartographic applications?
- Is a kite a suitable platform for a digital camera to map a small area?
- Is the quality of the obtained images good enough for use in ecological research?

The knowledge about the information contained in very high resolution images (below 10 cm. ground resolution) in ecological research is poor. Therefore, aspects that are not directly covered by the main objective or research questions will also be noted.

Methods

Study area

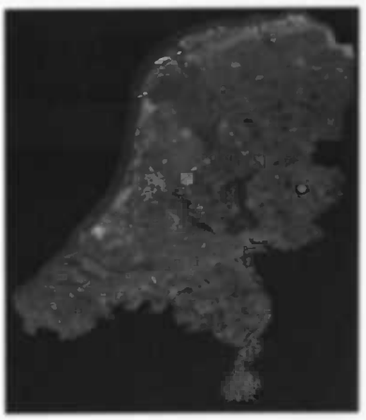

The study area is located in the east of the Netherlands The area is a nature reserve, managed by the Dutch forestry service. The landscape as it its today was formed during the Saalien glacial period (0.15 Ma B.P.) During this period the northern part of the Netherlands was covered with ice. At the peri-glacial, were ground is grinded, mixed and pushed upwards creating a hilly landscape (The Friezenberg, with an altitude of 40.2 meters is the highest point) with a mosaic of boulderclay layers. These impermeable clay layers prevented water from seeping through the soil, resulting in shallow pools where bogs (Elsenerveld en –veen) were formed.

The first signs of human activity are from 11.000 B.P. These early inhabitants left numerous burial hills in the area.

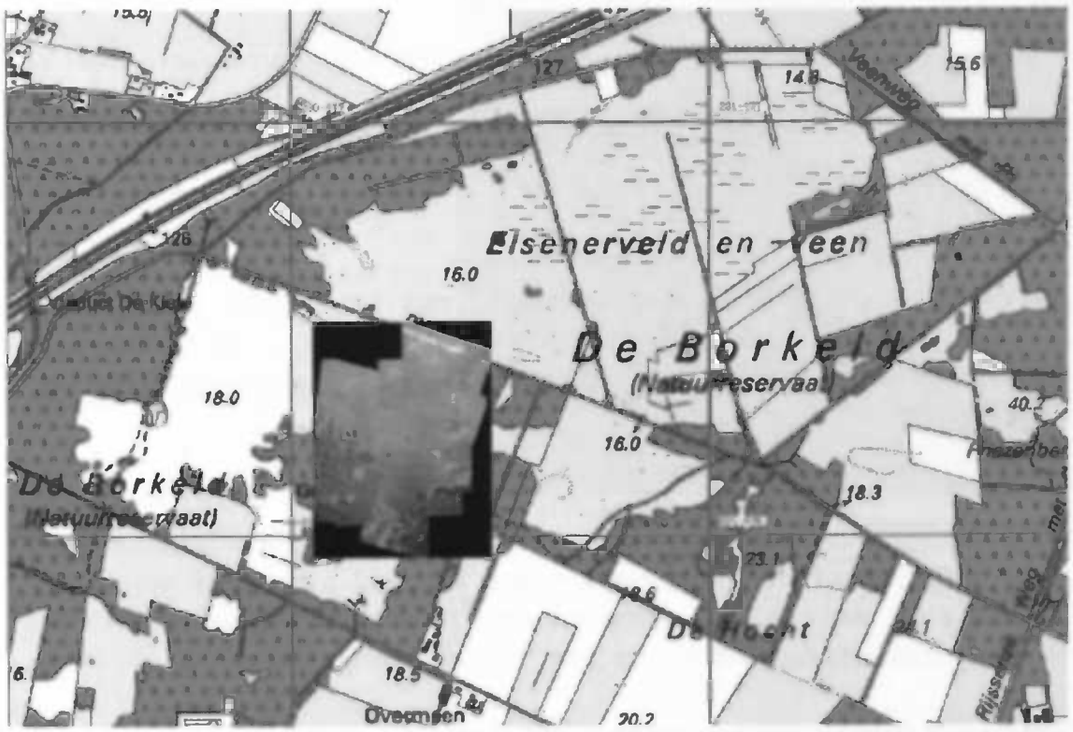

Figure 1: Research area; (RD coor. 464275, 230252) (lat,lon: 52.271265°, 6.491023°)
The grid cell size = 1 km^2.

Kite and lines

There are many different types of kites commercially available. Many are capable of lifting a camera. There are basically two types of kites. Soft foil kites and rigid kites.

Soft foil kites have no rigid structure or support to maintain their shape. The kite inflates with wind pressure and forms an airfoil profile, like the wing of an airplane, which provides substantial lift. Soft foil kites have several advantages for kite aerial photography. They have a very low weight-to-surface ratio, they are exceptionally easy to prepare and launch, and store just as easily; just stuff the kite into a small bag. For light-weight travel or backpacking, soft kites are the type of choice. Soft kites do have a tendency to collapse when the wind diminishes, so a watchful eye is necessary while in flight. As the name implies, rigid kites employ some type of hard framework to give the kite form and shape. Traditional supports of wood and bamboo are replaced in most modern kites by graphite rods and fibreglass poles, although wood and bamboo continue to serve a role in kite construction. Their weight-to-surface ratio is intrinsically greater than soft kites, but rigid kites do have some advantages for kite aerial photography (KAP). The primary advantage is the ability to fly well in light and gentle breezes without the danger of deflating and crashing. The frame maintains the kite's proper aerodynamic shape regardless of wind pressure. Although the frame can be disassembled, rigid kites can be troublesome for packing and travelling.

In this project the Power Sled Large, a semi-soft foil kite, was used. A semi-soft foil kite is a soft foil with very thin fibreglass elements that give some support to the canopy to prevent collapsing in light winds. The Power Sled Large dimensions are 2.40 m. x 1.13 m. and a surface of 2.7 m².

The kite is suitable for wind speeds between 2 and 5 Bft. (9 till 29 km/h.)

Because the kite generates a lot off force in stronger winds a heavy duty Dacron line with a breaking strength of 200 kg. is used.

Figure 2: The Power Sled Large in flight

Camera equipment and remote control unit.

Camera

The camera used in this research is a Canon s70. It is a compact 7.1 mega pixel camera. The camera has a shutter speed priority function and an IR remote control function (more camera info: www.dpreview.com)

Camera rig and suspension

To control the camera from the ground a special rig had to be build. Besides controlling the camera, the rig must also minimize camera movement. Many kite aerial photographers use a picavet suspension for their rig. The picavet suspension (1) keeps the camera, more or less, level to the ground independent from kite movement.

The camera rig operates on 2x2 AAA batteries (2). The switch (3) controls the power to the receiver (4). There are 2 servos for controlling the camera movement. One servo (5) is to change the camera view in oblique or nadir. The other servo (6) pans the camera 360°. Normally servos don't turn a 360° but after some slight modification in the servo's interior it does. The wire (7) is the infra red remote control that activates the shutter. It is attached to the front of the camera with some ducked tape.

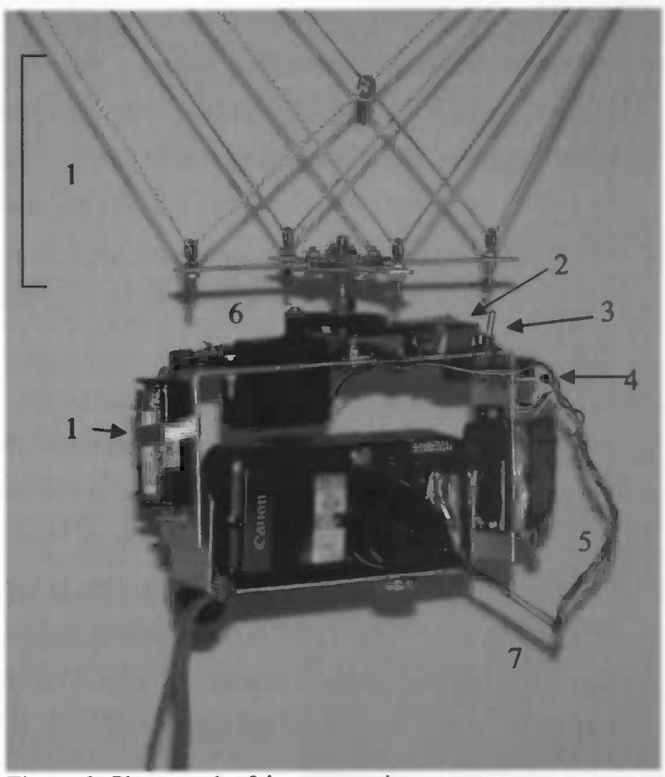

Figure 3: Photograph of the camera rig.

Remote control

To operate the camera from the ground a remote control for operating model airplanes was used (Futaba digital 4 channel remote control). There are 3 channels needed to operate the rig (ch.1 = 360° turn, ch.2 = oblique/nadir, ch.3 = shutter control)

The shutter is controlled by a Gentled. This is an infrared light emitting diode (LED) that is connected to the receiver and works on the IR remote control function of the camera. The shutter can be operated from the ground. The transmitter range in the open field is around 500 meters.

Taking the aerial photographs

When taking aerial photographs with a kite it is important to set the shutter speed of the camera as high as possible. It should be at least 1/250 second. This would still yield a considerable amount off blurred pictures. A shutter speed of 1/800 sec. or higher is preferred. When the lighting conditions are poor the sensitivity of the CCD can be increased by increasing the iso value. However this results in more noise in the images.

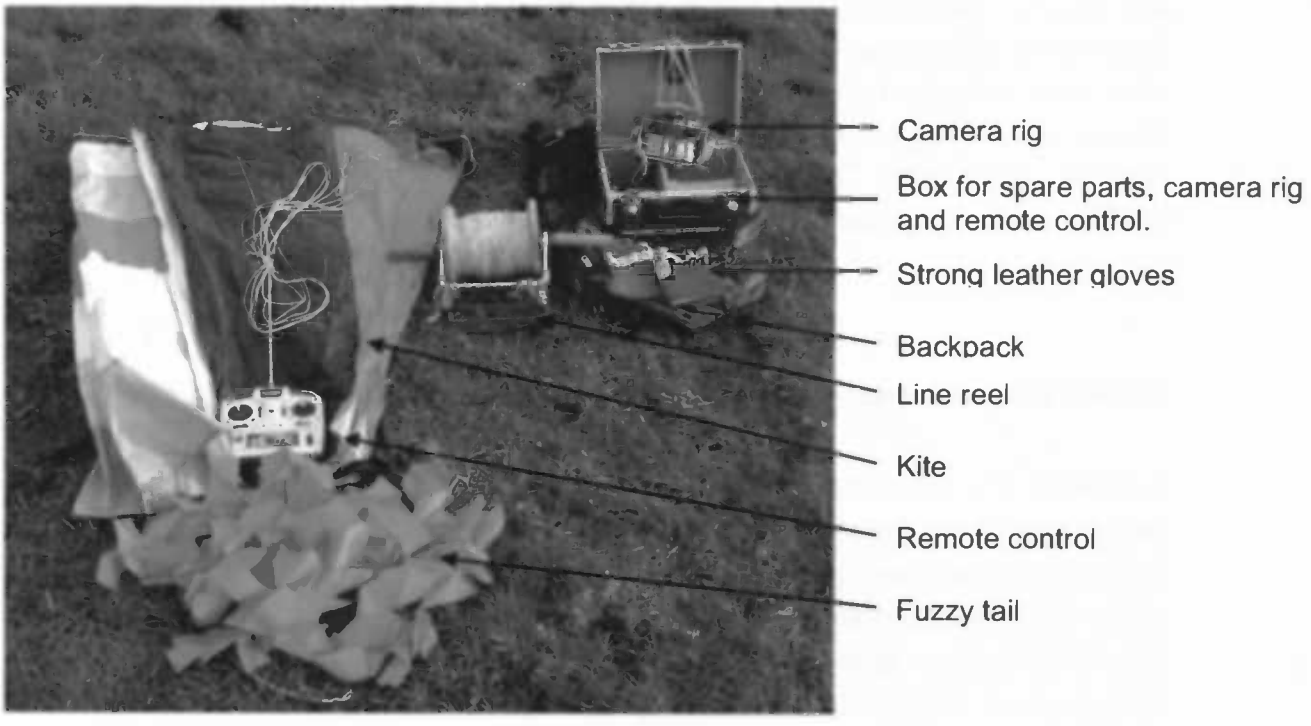

Figure 4: An overview of the kite equipment.

Figure 5: When the kite flies stable, the camera rig is attached to the line using 2 pieces of metal wire that are winded around the line. The distance between the kite and the rig is usually between the 20 and 50 meter.

Regulations and legal issues.

When flying a kite, the kite operator is responsible for its 'aerial vehicle'. This means that the operator should carefully examine the research area and equipment before flying. It should be avoided to fly near or over power lines and roads. One should also take care of other aerial vehicles. Airplanes are not allowed to fly below 150 meters, above build up areas planes have to stay above 500 meters. For flying below 100 meters, there are no regulations for kites, considered the kite is not within 5 km. of an airstrip. When flying above 100 meters it is good to notify air traffic control. They can send out an NOTAM (notice to airman). (Appendix 1)

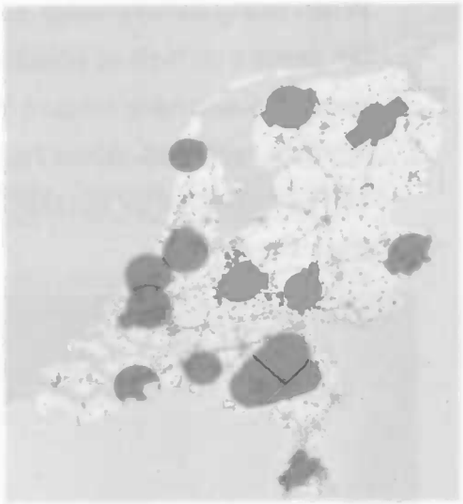

Figure 6: Red areas show the locations of airstrips. In these area's it is not allowed to fly a kite. Source: air traffic control Netherlands

Ground control points.

To define the geometric transformation process it is necessary to have several ground control points that are visible on the photos. Ground control points are points with known coordinates. These coordinates can be absolute or relative. Absolute coordinates give a position that is in a geographical projection. E.g. Latitude, longitude coordinates or RD (rijksdriehoeks) coordinates. Relative coordinates are points with known positions in relation to each other but are not linked to a geographical projection. In this study the RD coordinates are used.
The ground control points are measured with the Leica 1200 GPS. This is a kinematic phase differential gps that is used for high precision geodetic measurements.
As ground marks large A3 white paper sheets were used. The sheets had a large black spot, of which in the middle the coordinates were measured. There was also a number printed on the sheet for easy identification (Figure 8).

Figure 7: Jan Hendriks in the field with the Leica 1200

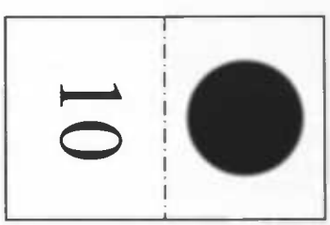

Figure 8: Example ground mark.

Calibration of non-metric digital cameras

In conventional aerial photography so called 'metric' cameras are used. Metric cameras have a known interior orientation. The focal length, pixel size, principal point and lens distortion parameters have been determined so it can be used for photogrammetic work. Since consumer digital cameras are not metric, the camera parameters have to be determined (Chandler, 2005).

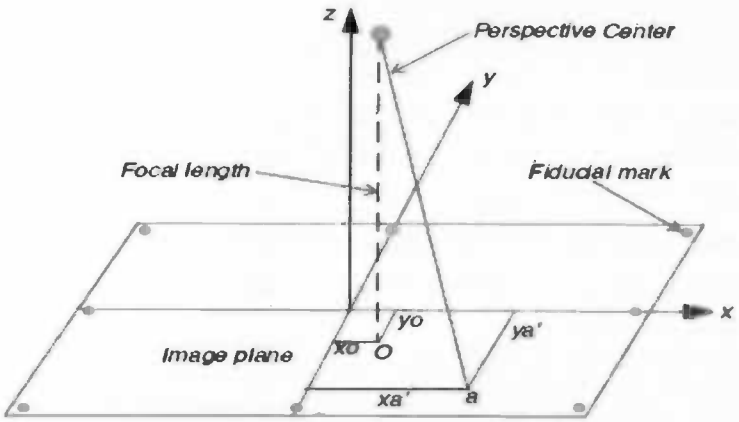

Figure 9: The focal length is the distance from the image plane to the lens center. The principal point is the location on the image plane where the optical centre of the lens crosses.

Focal length and pixel size can be calculated from the camera specifications. Principal point and lens distortion are a little more difficult to determine. Lens distortion deteriorates the positional accuracy of image points located on the image plane. It is visible when photographing a raster with an equal distribution of lines (Figure 10). When viewing the image on a print or computer screen the square will appear deformed, suffering from pincushion or from barrel distortion (Figure 11). The Canon s70 has a wide angle lens (28mm equivalent). This means that it has a wide field of view and hence, it can cover more ground in one aerial photo then a camera with a smaller field of view.

Figure 10: Photograph of a raster taken with Canon s70. The barrel distortion is obvious, especially in the corners. The corners also appear darker then the rest of the image

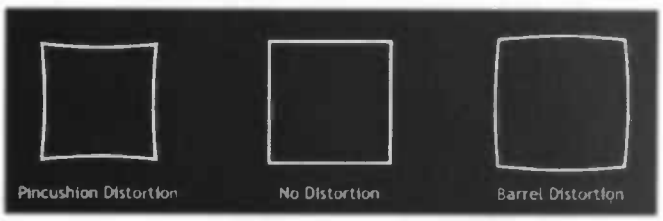

Figure 11: Effects of lens distortion.

The radial lens distortion is described by two parameters, radial and tangential lens distortion (Figure 12). The tangential distortion can be neglected it in this case. The effects of radial lens distortion throughout an image can be approximated using a polynomial function.

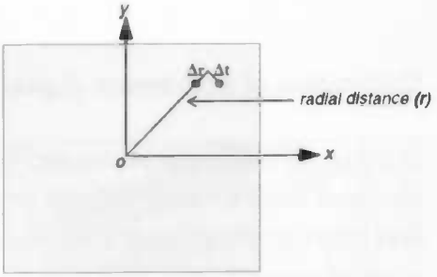

Figure 12: The radial distortion Δr and the tangential distortion Δt as a function of the distance (r) from the principal point.

There are several methods to determine the camera calibration parameters. In this case Photomodeler 5 was the best choice. It is a software package that uses consumer digital camera's to create 3d models of objects. It is used in accident reconstruction and cultural heritage archiving. The software has a full calibration mode that produces data about focal length, principal point, ccd-chip size, pixel size and lens distortion parameters. Photomodeler 5 uses the following polynomial for radial lens distortion (equation 1):

$$\textit{Equation (1):} \qquad \Delta r = (k1)r^2+(k2)r^4+(k3)r^6$$

Erdas Leica photogrammetic suite (8.7).

To process the kite aerial imagery Leica photogrammetic suite (LPS) was used. LPS is an addition to ERDAS GIS software. The software uses the ground control points from the GPS and tie points (points that are on two or more images but without known coordinates) to calculate by triangulation the position of the camera, and from there it geo-rectifies the aerial images. Since a lot of images overlap it was also possible to extract a digital elevation model. The software needs the camera parameters for accurate geo-rectification. LPS uses different parameters for the lens distortion (equation 2):

$$\textit{Equation (2):} \qquad \Delta r = (k0)r+(k1)r^3+(k2)r^5$$

A conversion table was created in Excel to use the parameters from Photomodeler 5 in LPS.

Vegetation survey

To collect ground data, 30 plots (2 m. x 2 m.) were selected within the mosaic map area. Within each plot the cover percentage of the dominant plant species were recorded the average canopy height.

Image classification.

The high resolution images will be visual and computer-aided classified in to different classes. The vegetation types or characteristics of each class have to be determined in such way that they can be distinguished by the human eye and the computer. For the computer-aided classification, representative pixels of each class need to be selected to serve as training data for the software.

Results

Camera calibration

The basic camera parameters are summarized in Table 1. The canon s70 that was used has a 28 mm equivalent lens which is a wide angle lens. Although this delivers a large ground coverage there is more distortion in the corner of the images.

Field Of View X (°)	Field Of View Y (°)	sensor size s70 X (mm)	Y (mm)	Amount of pixels X	Y	Pixel size On ccd-chip(µm)	Focal length (mm)
63	47	7.18	5.32	3072	2304	2.3	5.8

Table 1: Camera parameters based on Canon Datasheet. The pixel size on the ccd-chip is derived by dividing the sensor size by the amount of pixels.

Based on the field of view and the pixel size on the chip, the coverage and ground resolution of an image with respect to the flying height was calculated (Table 2).

Height	X (m)	Y (m)	m²	Ha	Ground resolution (cm)
50	61.3	43.5	2664.5	0.3	2
100	122.6	87.0	10658.1	1.1	4
150	183.8	130.4	23980.8	2.4	6
175	214.5	152.2	32640.5	3.3	7
200	245.1	173.9	42632.5	4.3	8
225	275.8	195.7	53956.8	5.4	9
250	306.4	217.4	66613.3	6.7	10

Table 2: The ground coverage and resolution of a single image with respect to the flying height.

With Photomodeler 5 the lens distortion is determined by photographing a calibration sheet from multiple angles. The calibration sheet has a regular grid of point's which the software automatically detects on the photographs.
The values for K0, K1 and K2 are: 7.110e-003, -5.360e-004, 2.122e-005. For use in the LPS software module the output of Photomodeler needs to be recalculated.

The lens distortion in the principle point is zero (Figure 13). The distortion increases when the distance from the principal point increases. overview of the calibration parameters is in appendix 2

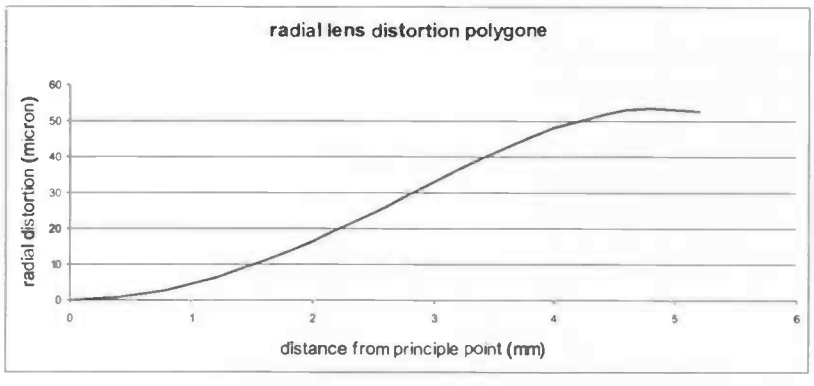

Figure 13: Graph of the polynomial function as used in LPS

Ground control points

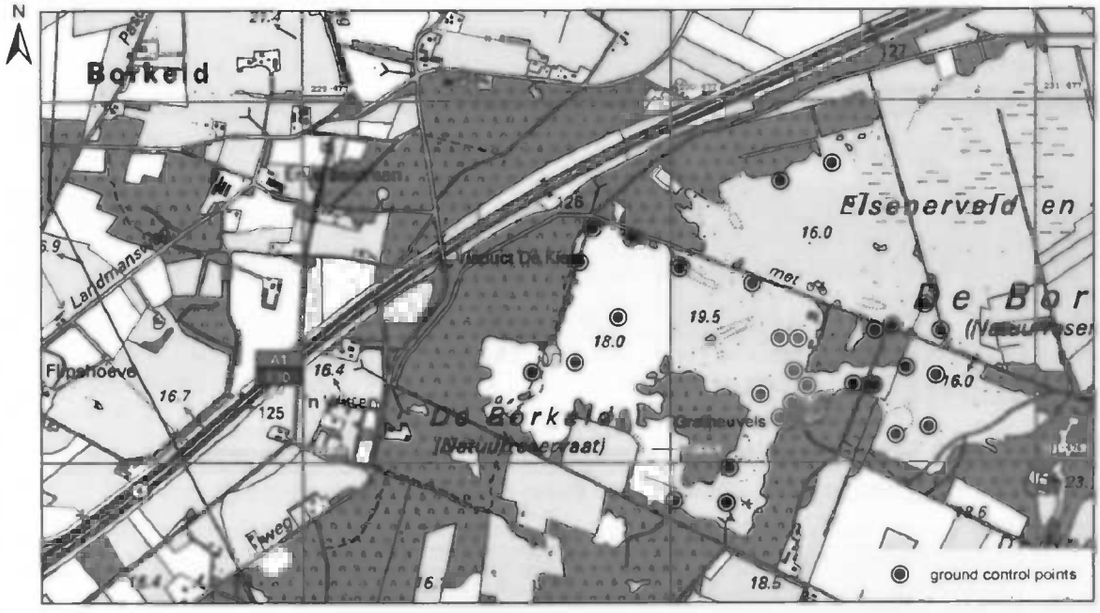

Figure 14: location of 37 measured ground control points. The points in red were used for the mosaicing procces.

The ground control points (GCP's) measured with the Leica 1200 gps had an overall accuracy of 2 cm. in horizontal plane and 4 cm. in vertical plane. A complete list of the GCP's and their accuracies is in

Appendix 2: Camera Calibration Photomodeler 5 Status Report Tree

Information from most recent processing	Quality
FocalLength Value: 5.965779 mm Deviation: Focal: 0.004 mm Xp - principal point x Value: 3.539505 mm Deviation: Xp: 0.008 mm Yp - principal point y Value: 2.663596 mm Deviation: Yp: 0.007 mm Fw - format width Value: 7.188917 mm Deviation: Fw: 0.004 mm Fh - format height Value: 5.410200 mm K1 - radial distortion 1 Value: 7.110e-003 Deviation: K1: 4.4e-005 K2 - radial distortion 2 Value: -5.360e-004 Deviation: K2: 3.2e-006 K3 - radial distortion 3 Value: 2.122e-005 P1 - decentering distortion 1 Value: -3.080e-004 Deviation: P1: 4.3e-005 P2 - decentering distortion 2 Value: -6.903e-005 Deviation: P2: 4.1e-005	Photographs Total Number: 8 OK Photos: 8 Number Oriented: 8 Cameras Camera1: canon s70 Calibration: yes Number of photos using camera: 8 Point Marking Residuals Overall RMS: 0.318 pixels Maximum: 3.198 pixels Point 100 on Photo 1 Minimum: 0.183 pixels Point 10 on Photo 8 Maximum RMS: 1.480 pixels Point 100 Minimum RMS: 0.098 pixels Point 54 Point Precisions Overall RMS Vector Length: 0.000283 m Maximum Vector Length: 0.000449 m Point 100 Minimum Vector Length: 0.000219 m Point 48 Maximum X: 0.00029 m Maximum Y: 0.000286 m Maximum Z: 0.00022 m Minimum X: 8.73e-005 m Minimum Y: 9.03e-005 m Minimum Z: 0.000155 m

Appendix 3:

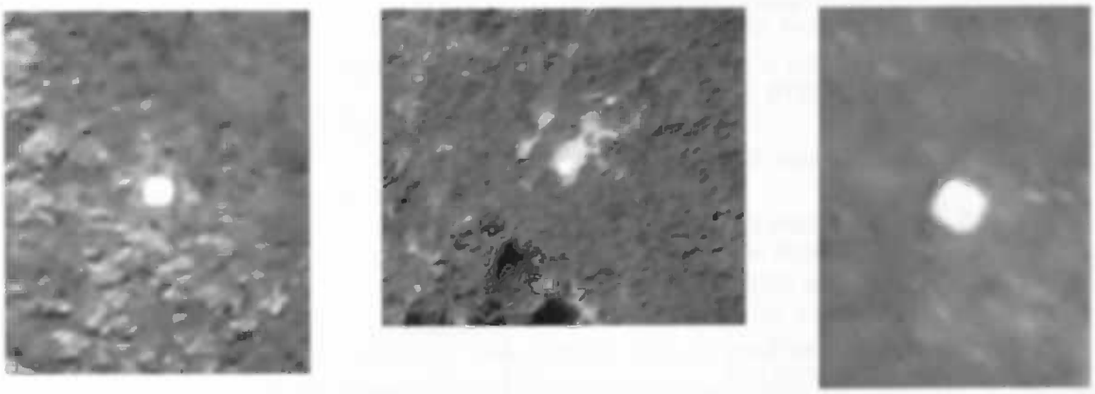

Figure 15: Ground control markers

The A3 paper sheets that were used as ground control marks were large enough to be detected on the images. However the reflection of the white paper was so strong that it overcastted the black circle and number (Figure 15). This blooming effect caused inaccuracy in the final image mosaic because the GPS coordinates were based on the centre of the black spot. For further processing the ground control point coordinates were linked to the centre of the A3 sheet. This caused an inaccuracy of ± 15 cm. Another effect that is visible is (purple) fringing, an effect that often occurs when a ccd is confronted with highly contrasting light.

Base map

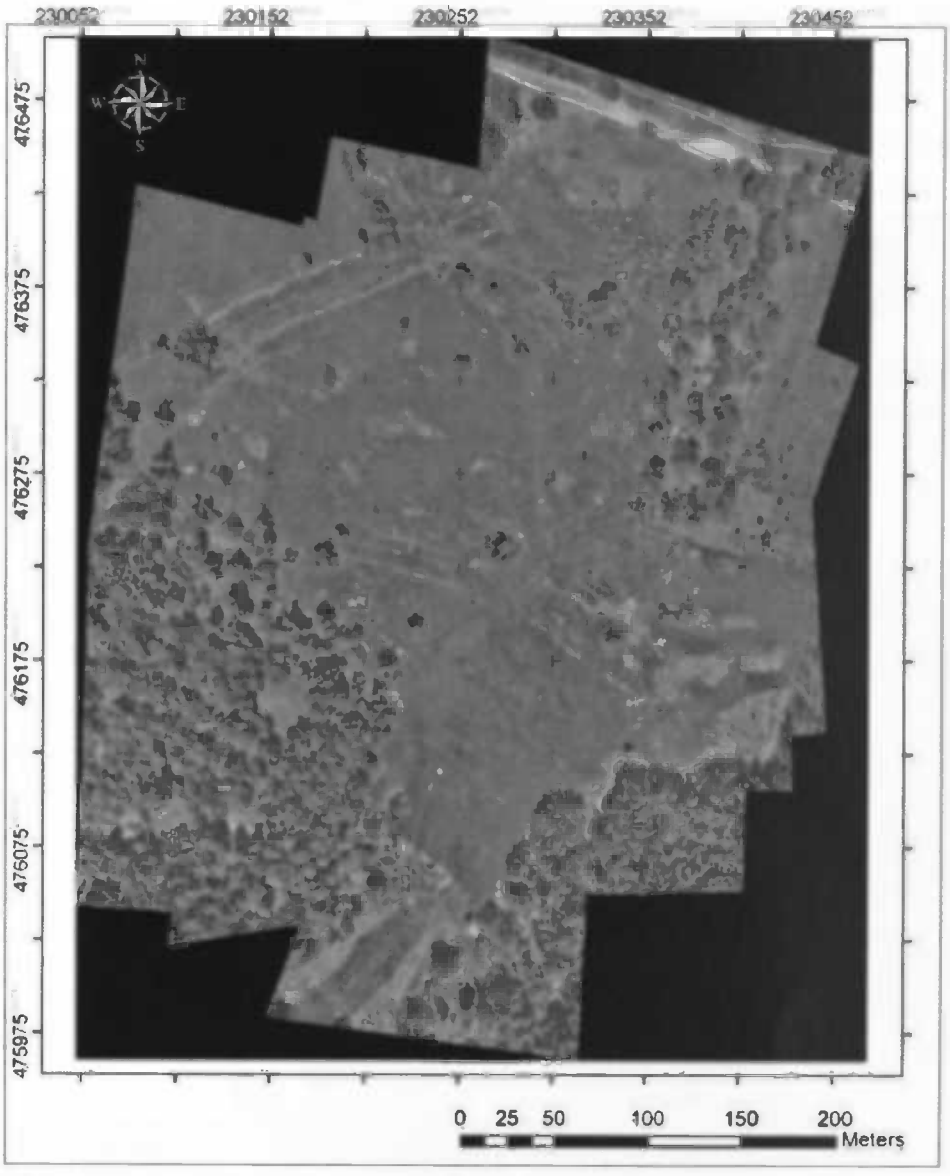

Figure 16: Resulting mosaic image. The mosaic is built up from 16 individual images

The result of the photo mosaicing is shown in Figure 16. The area covers 16.9 hectare. The original images have a ground resolution between 2 and 8 cm. After the mosaicing operation and resampling the ground resolution is 9 cm. The mosaic smoothing operation (histogram matching, and cutline dodging) did a good job for the final result. There are however some areas where cutlines are visible and there are some unsharp regions.

The total image root mean square error for the triangulation is 0.6311. The total image RMSE depicts the quality of the entire triangulation solution in pixels.

Exterior orientation results.

The triangulation results show the calculated camera positions and angle for each image. The altitude at which the images are taken varies between 145 and 207 meters. In appendix 4 the exact locations, altitude, yaw, pitch and roll off the camera at the time a photo was taken.

Vegetation classification.

Visual image interpretation/ classification.

The high resolution of the kite aerial images is very suitable for visual interpretation of the features seen on the ground. The human eye is able to relate colours and patterns in an intuitive way that no computer software can match (itc textbook, 2004)

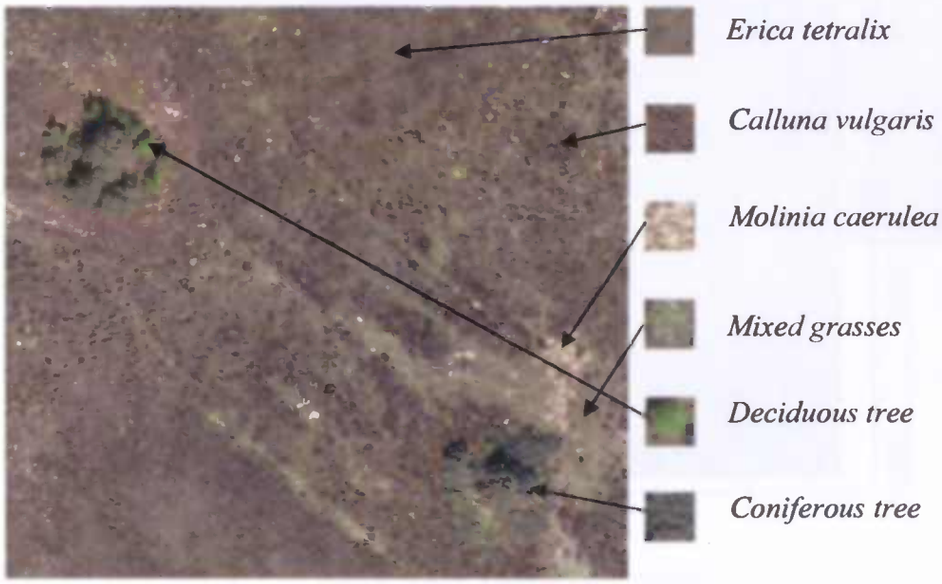

Figure 17: Cut out section off base map

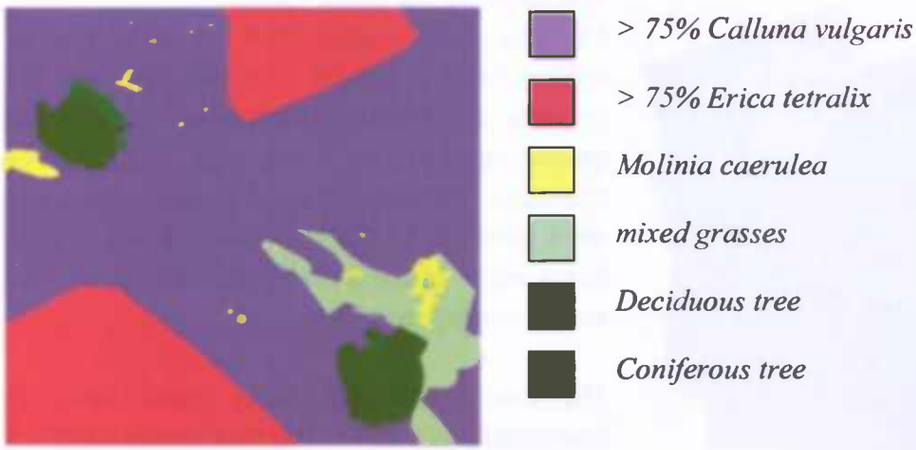

Figure 18: Result of visual interpretation of aerial photograph

Vegetation survey

The high resolution map can be used in the field to locate the positions of plots that were surveyed. The maps below show the distribution of the vegetation survey points. Map 1 till 5 shows the abundance of the most occurring ground cover types.

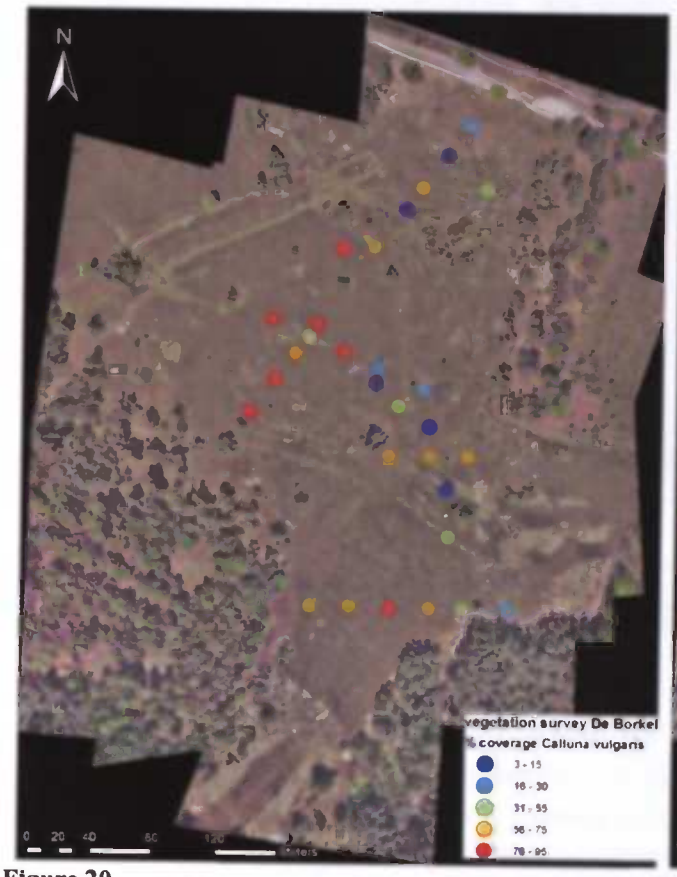

Figure 20

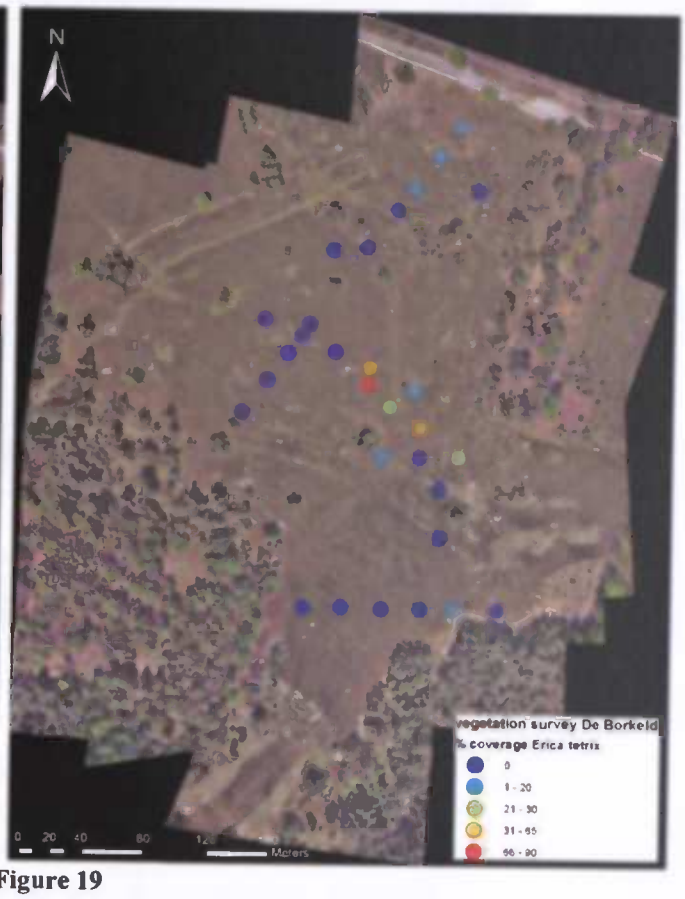

Figure 19

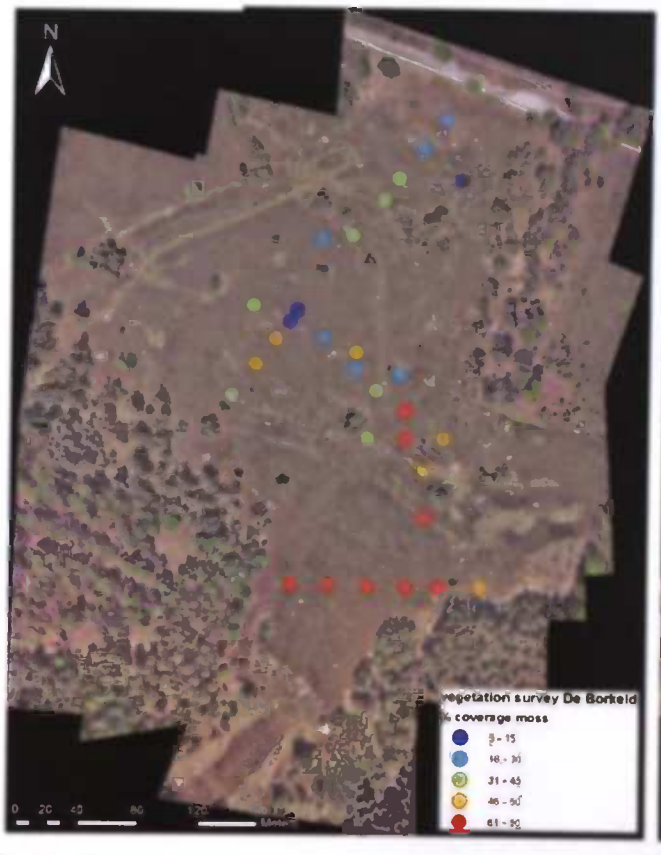

Figure 23

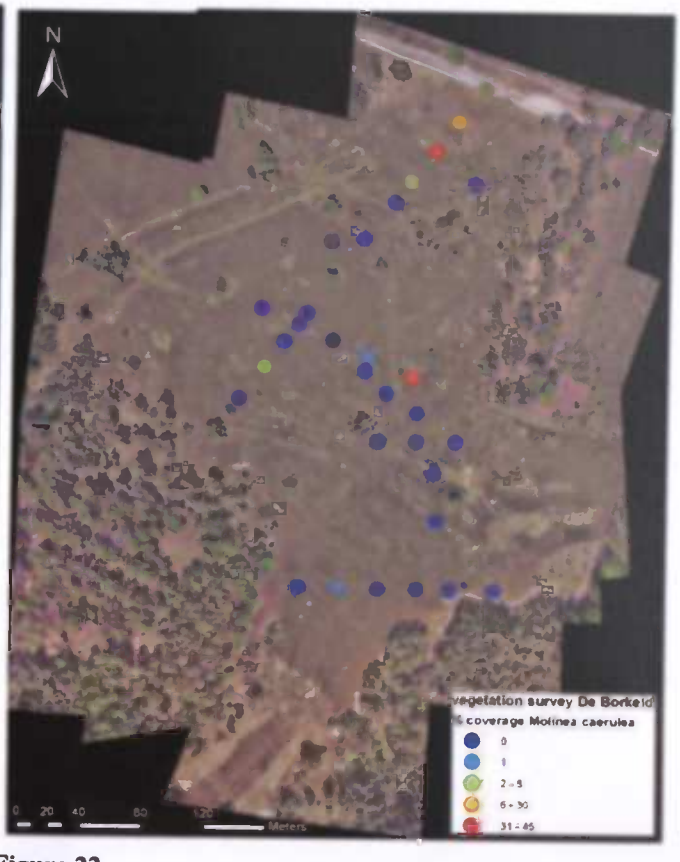

Figure 22

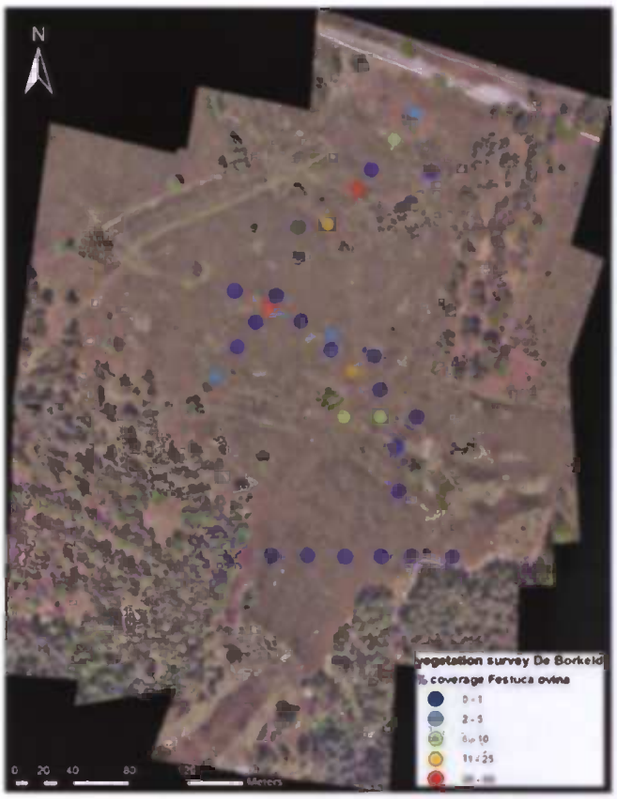

Figure 24

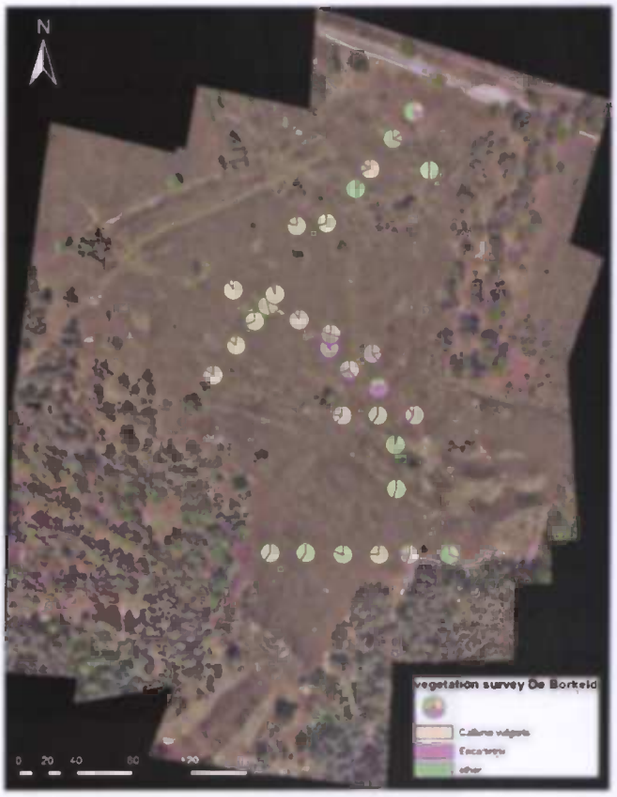

Figure 25

Supervised classification.
Supervised classification is a process where pixel values are linked to a ground cover class. The quality of the classification depends on the separability of the different pixel values from each class. In this case 5 classes were chosen that are easily distinguishable by eye on the base map.

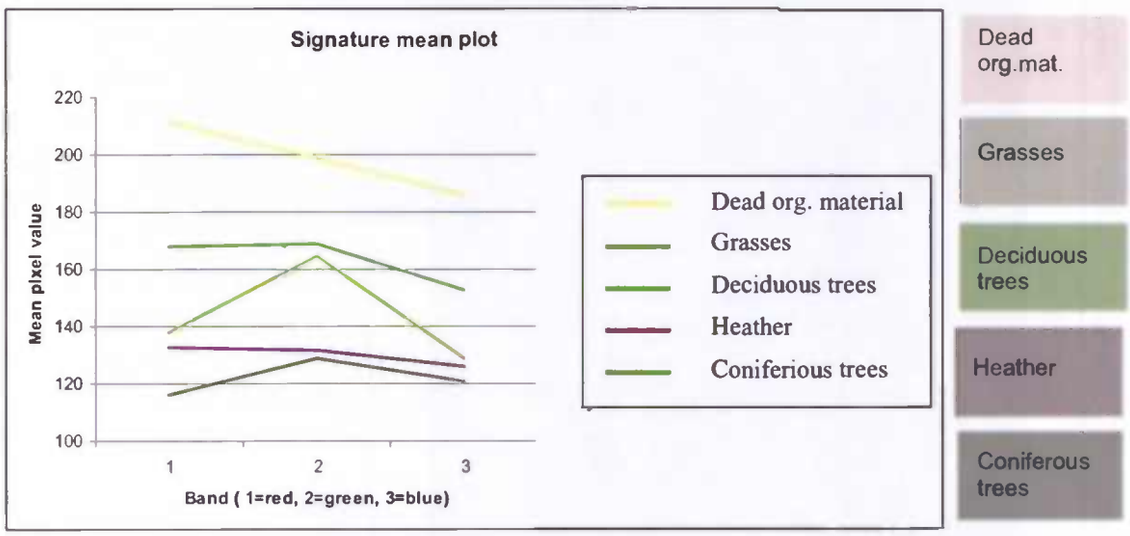

Figure 26: Signatures means of the 5 different classes. The squares beside the graph show the actual colors of the classes as they are seen in the mosaic.

The signatures are based on the pixel values from the three bands that are available in a consumer digital camera. The bands are depicted on the X-axis. The largest variety in pixel values between the 5 classes is in the red band. In the green band (2) the deciduous and grasses are close together as are the heather and coniferous type. The signatures of heather and coniferous trees are close together, which isn't surprising since the leaves of *Calluna vulgaris* are dark green, almost the same as from coniferous trees. The spectral signatures are so close together that it could give problems in the classification. The class dead organic material shouldn't give any problems since it is highly separated from the rest of the classes however it must be taken into account that bare sandy soil and footpaths also have a high reflectance.

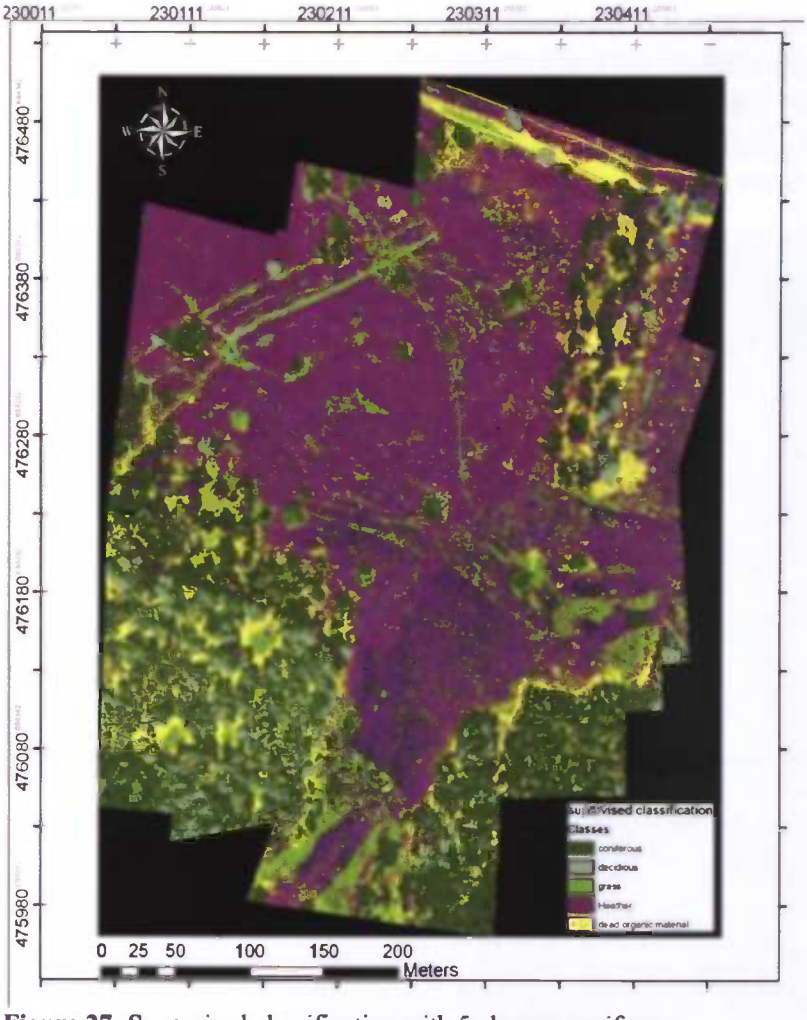

Figure 27: Supervised classification with 5 classes; coniferous, deciduous, grass, heather and dead organic material. Classification is based on the signatures shown in Figure 26

The result of the supervised classification looks good, based on visual inspection. There are however certain areas where pixels are assigned to the wrong class. For instance the edges of most of the deciduous trees are classified as coniferous type and visa versa. This is caused by shadows and light variations. Some grass areas are classified as deciduous, due to the same reason.

The total coverage of the different classes is shown in Figure 28.

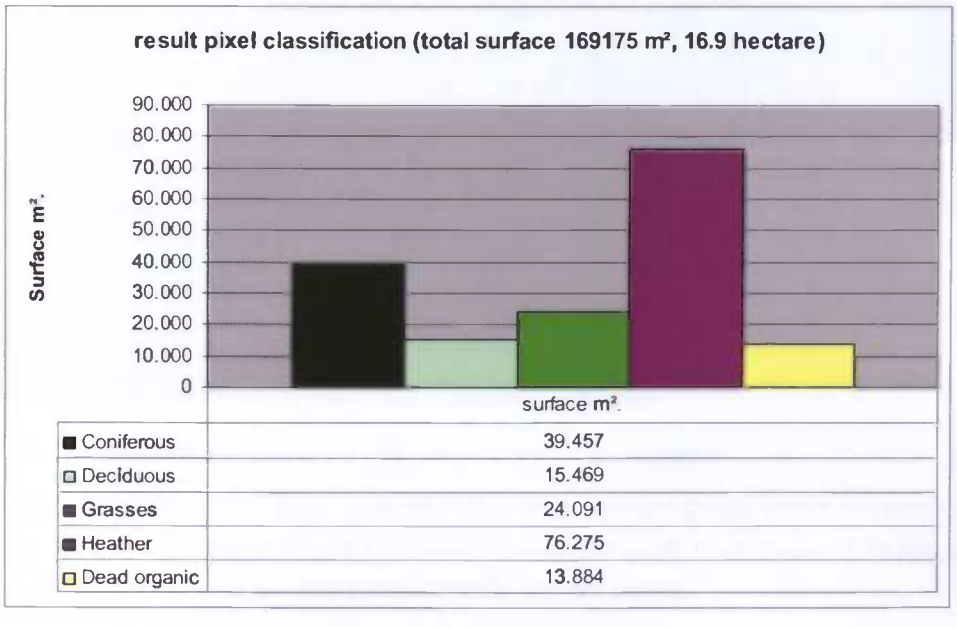

Figure 28: The result of the supervised classification.

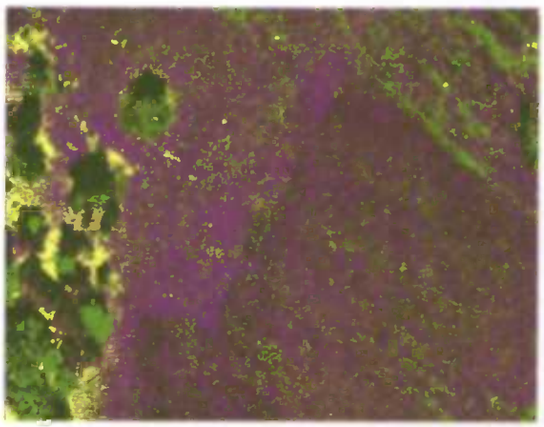

Figure 29: Section of Figure 27.

In Figure 29 a section of the classification map is displayed. The centre of the section shows a heather area. Within the heather a lot of pixels are classified as coniferous and deciduous tree type. This is a misclassification, but it basically means there are a lot of pixels with spectral signatures similar to that of the coniferous and deciduous tree. When looking at the moss distribution in the heather the amount off moss coverage is between 60 and 80 percent in this area. This could account for the high amount of 'greenness'. Another probability is that the "greenness" is caused by a higher vitality of *Calluna*. The boundary that is visible from the bottom left to the upper right is likely to be an artefact from the image mosaicing process.

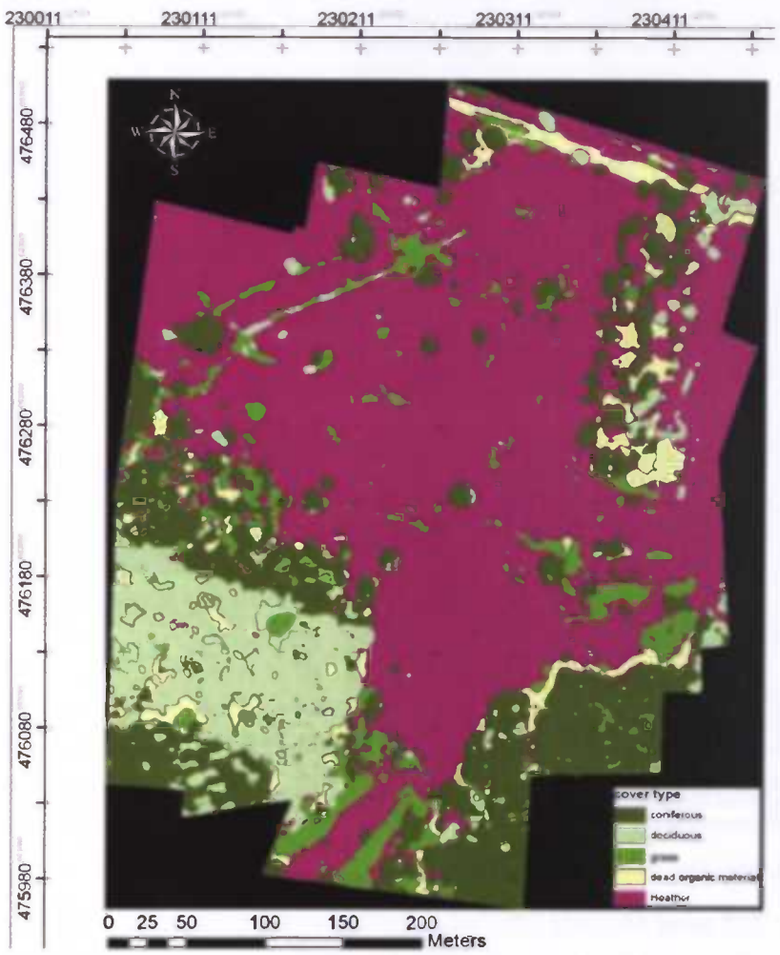

To create a more uniform map a majority filter was applied. A majority filter checks in a certain matrix e.g. 3x3 pixels or 5x5 pixels which land cover type occurs most frequently and assigns this type to the whole matrix. This reduces the speckled or dotted appearance as in Figure 29.
The result is in Figure 30
The majority filter was constructed in Erdas modelmaker. The majority filter setup is in appendix 5.

Figure 30: Classified map after applying a 51x51 majority filter.

When looking at the basemap there are several areas visible with a high (>75% coverage) abundance of *Erica tetralix*. The spectral signatures of both heather types are very similar. In order to identify these areas, the heather area was clipped out of the basemap. The resulting map was classified using the spectral signatures of two classes; *Calluna vulgaris* and *Erica tetralix*.

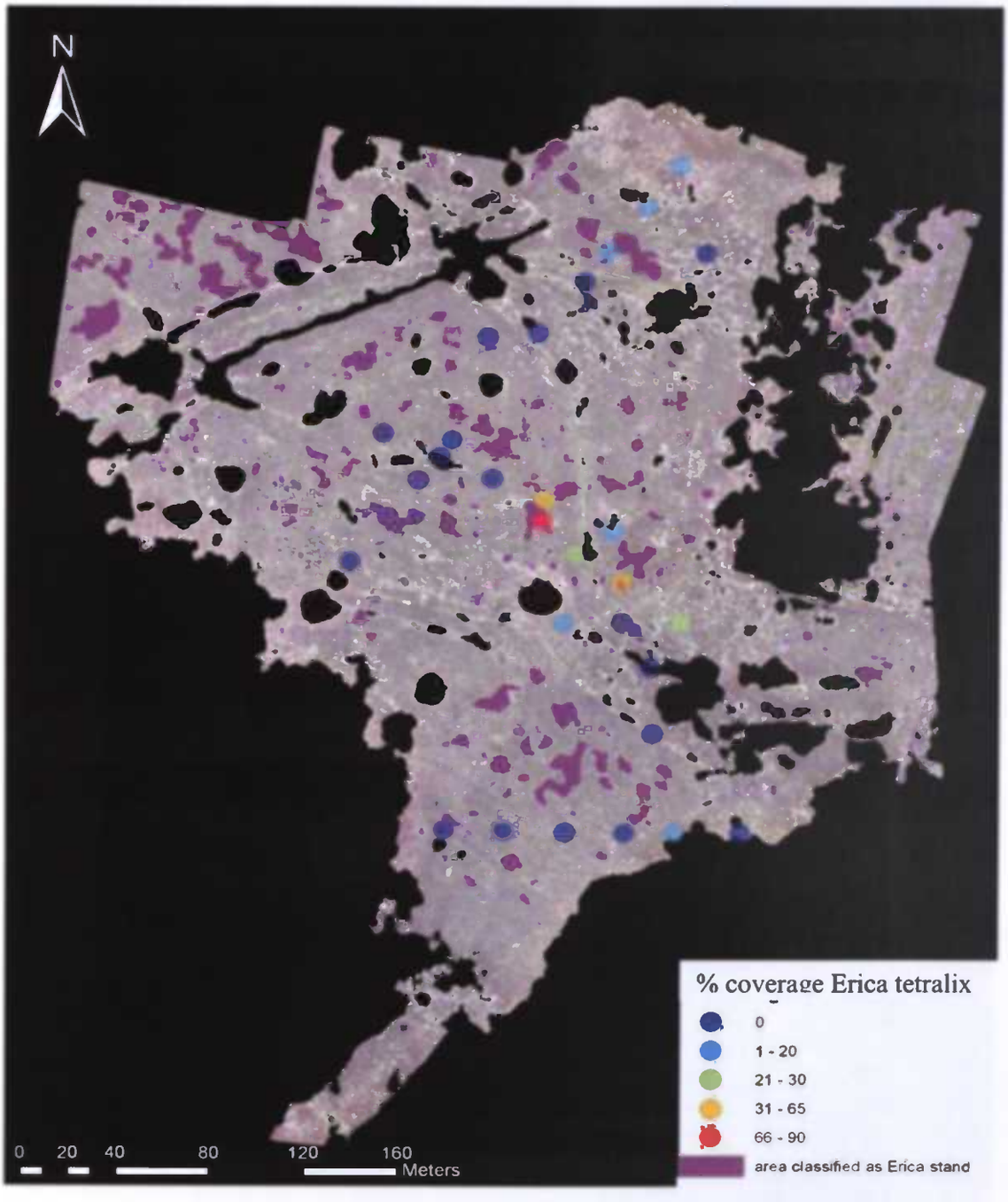

Figure 31: Areas with a high probability *on Erica tetralix* stands are in purple.

After the classification a 3x3 pixel majority filter was applied three times to remove all the small patches and single pixels that were classified as *Erica tetralix*. The resulting map predicts where the larger are *Erica tetralix* stands occur.

Digital elevation model

With Orthobase Pro a Digital Elevation Model was constructed using 4 overlapping images. The horizontal resolution is 20 cm. The average ground level is 19.6 meters above DOL. (Dutch Ordnance level). The mean error based on 23 control points is -0.04 m (appendix 6). The higher (yellow to red) areas are trees which clearly stands out above the surface of the model.

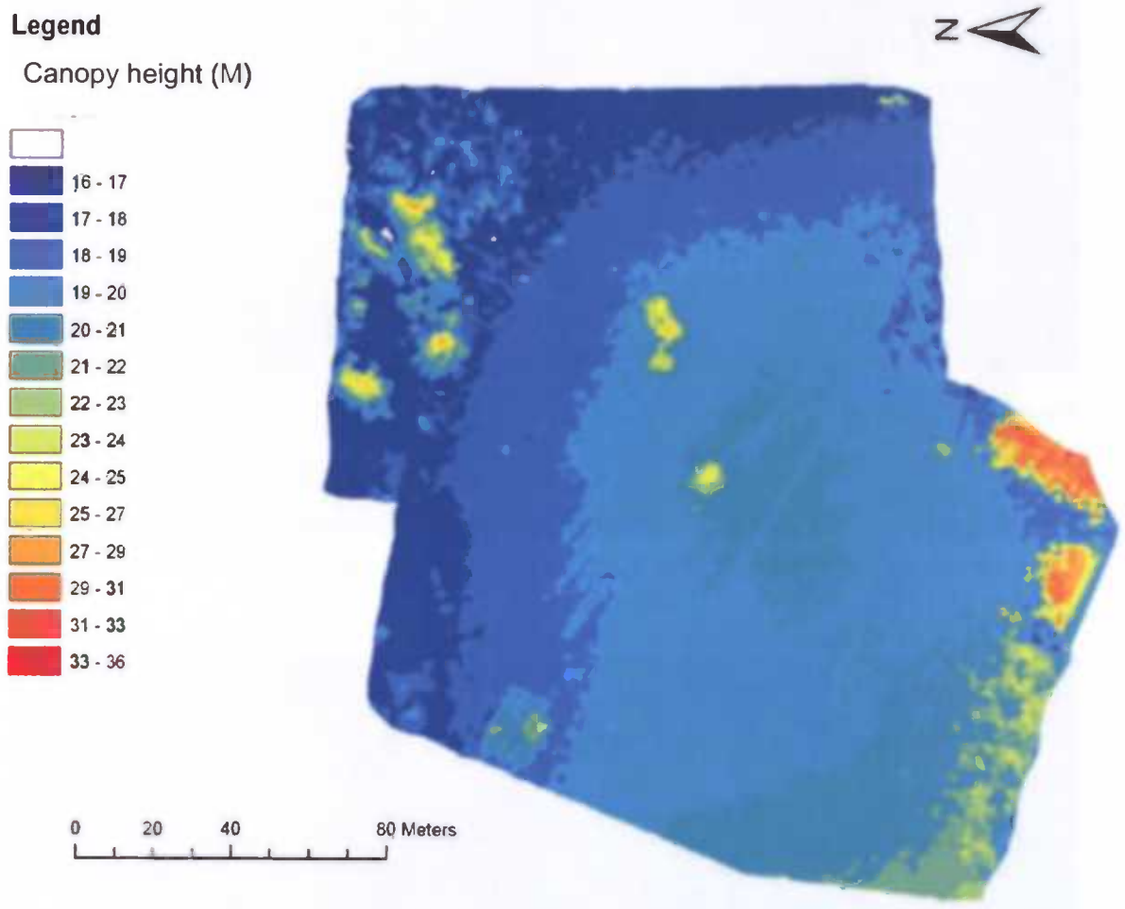

Figure 32: Digital elevation model from kite aerial images.

Around the bottom right edge the DEM extraction went wrong. This area is a normal flat heather surface, but the in the DEM this is a relatively heterogeneous area. This could have been caused by a local heather roughness or structure which makes it hard for the software to find similar points on the different images. The overall height shows a decrease from the bottom right to the upper left corner, which agrees with a 5 meters resolution radar DEM of the same area.

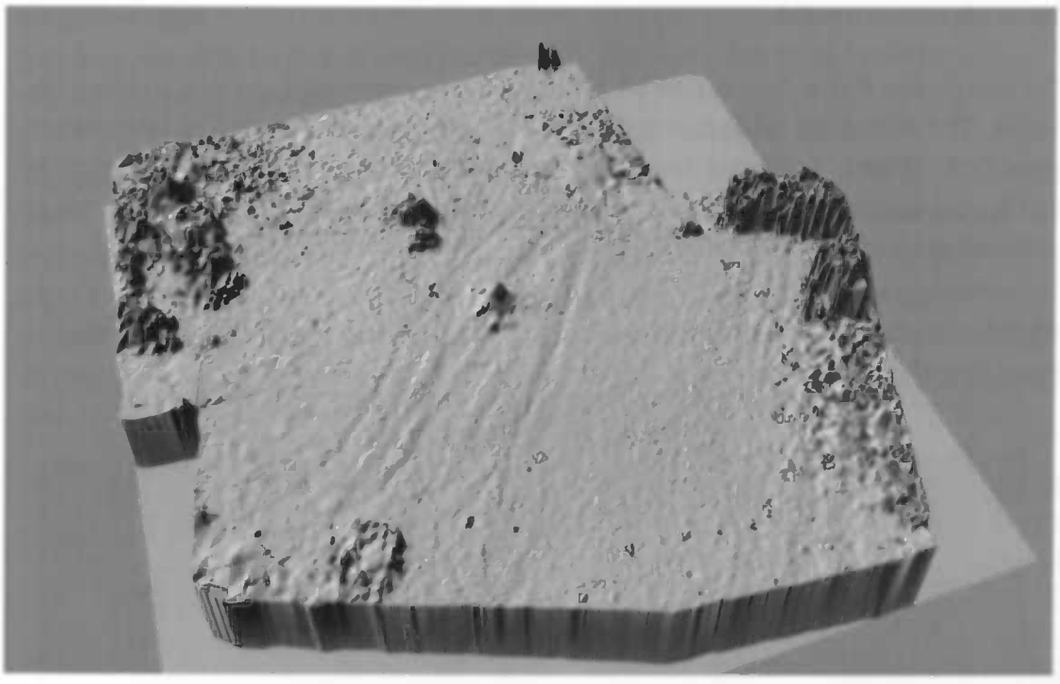

Figure 33: 3d model created with kite aerial images.

When displaying the DEM in a 3d viewer the surface details become visible. The small gully's are clearly visible in the model. When displayed with a mosaic image on top we see that at the location of the gully's match with the grass patterns.

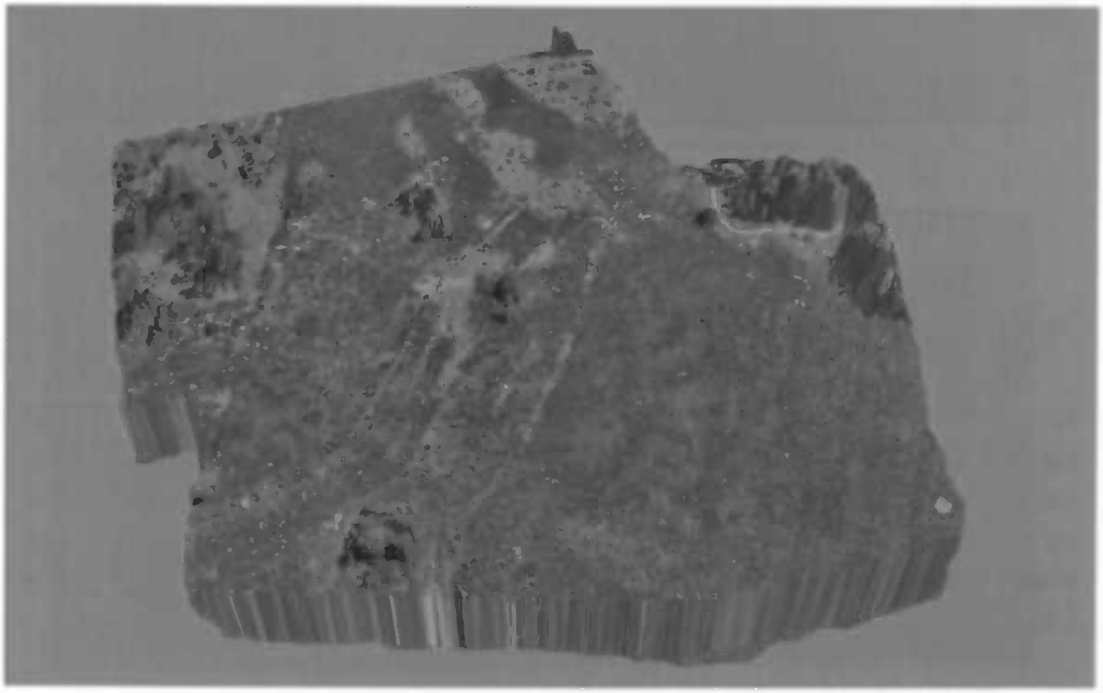

Figure 34: Same model as Figure 32 but with image overlay.

Height profiles

In the graphs below detailed elevation profiles from a cross section through the gullies is shown.

Figure 35: location of the elevation profiles. Red arrow is shown in Figure 36. The bleu arrow is shown in Figure 37

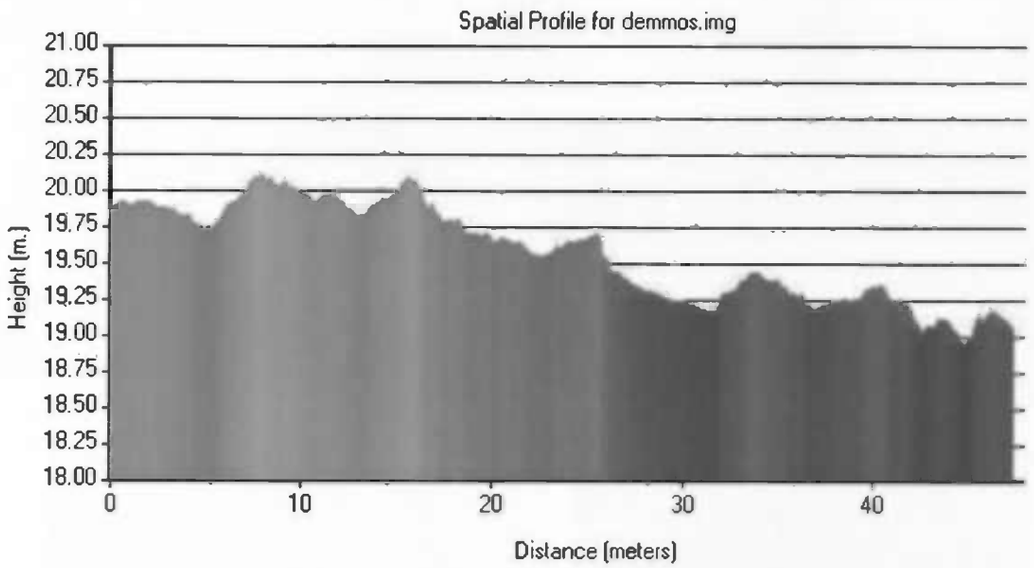

Figure 36: Elevation profile through the gullies. The red arrow shows the position of the profile.

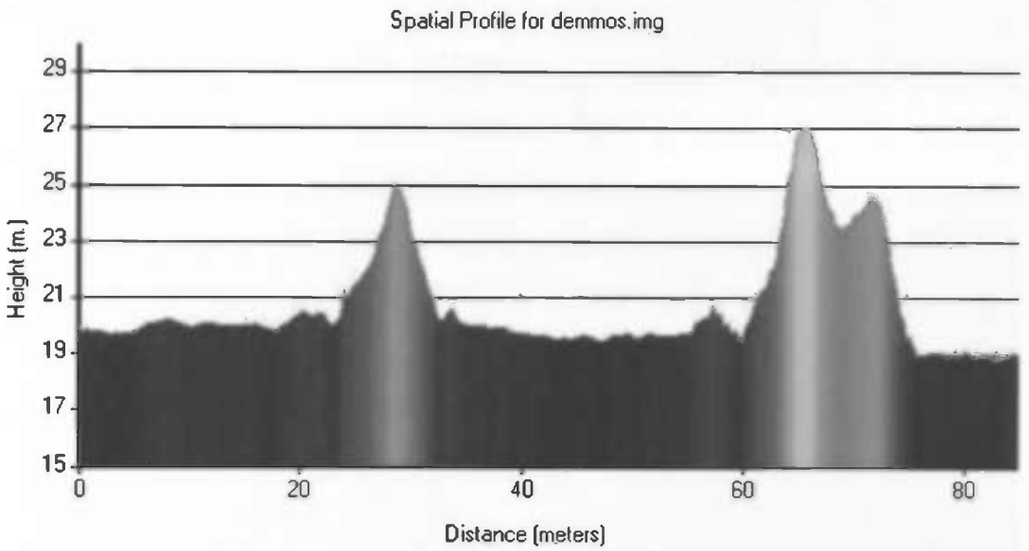

Figure 37: Elevation profile (blue arrow) through the trees. Based on this the height of the trees can be determined. The first tree is ± 5 meter high and the other one is ± 7 meter.

Miscellaneous

Below are several items that aren't covered by the main objectives or research questions though they are worth mentioning.

Temporal resolution

The spectral characteristics of features change over time. Figure 34 shows two images taken on different dates. The left image, taken on 9 May clearly shows patches of *Molinia Caerulea.* In the image taken on 1 September these patches are hard to distinguish from the other vegetation. The image taken in September on the other hand shows flowering heather and could be used to create a heather health map.

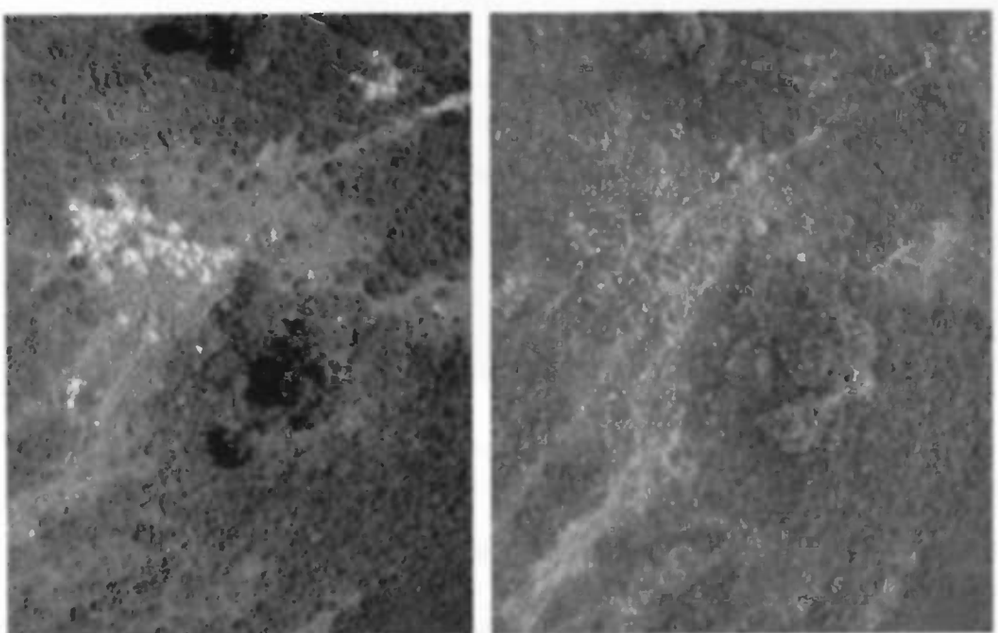

Figure 34: Two images of the same area. The left I images is taken on 9 May 2006, the right image on 1 September 2006.

Figure 35: Mosaic of two images taken on 1 September. The camera is looking to the west. The area's with a high coverage of Erica tetralix (grayish patches on foreground) are distinguishable from the area's with a high coverage of Calluna (more purplish central area). Pine tree seedlings that will slowly overgrow the heather area are chopped down and left on the spot (brown dots).There are however many seedlings that still have to be chopped (the many green dots)

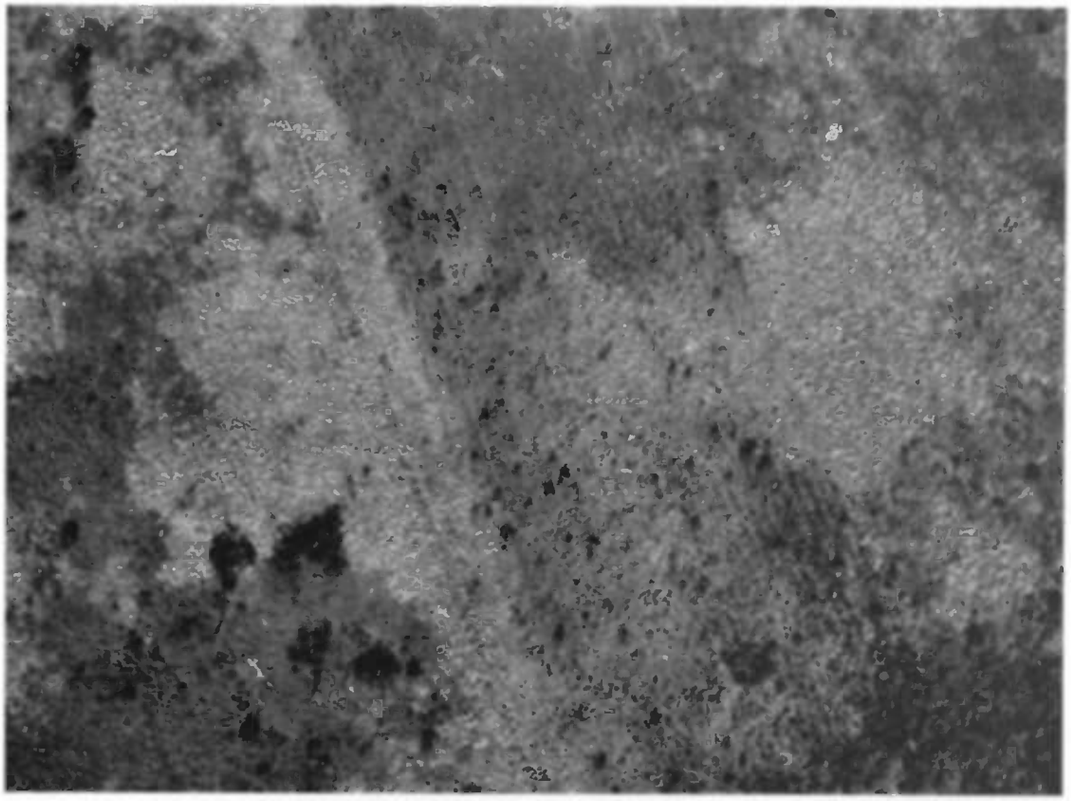

Figure 36: Photograph taken on 12 June. The heathland area suffers from grass invasion. After mowing the heather has more or less re-established itself. Besides the heather, pine tree seedlings also profit from this management regime.

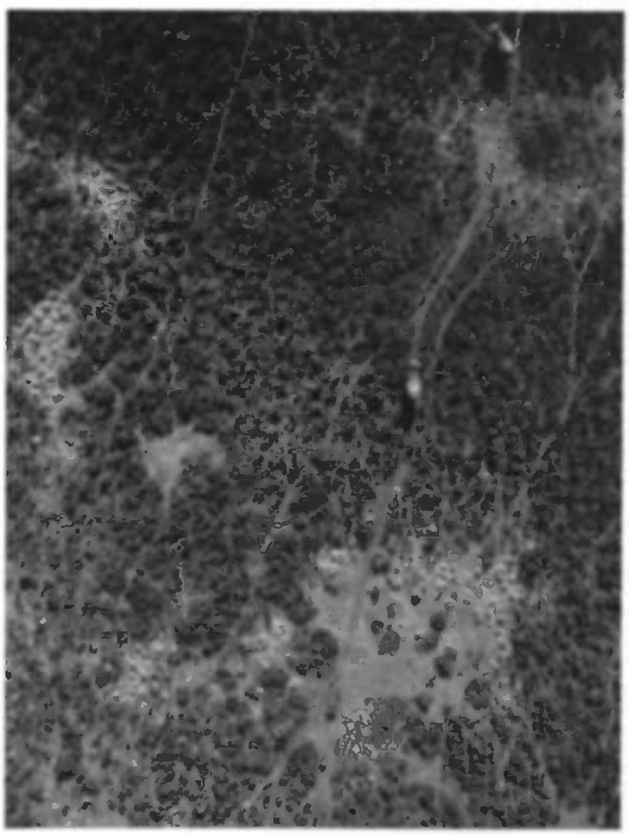

Figure 37: This image is taken at 'Noordsche Veld'. A nature reserve near Assen.

Figure 38: Kite aerial images show with high detail the tracks of animals that cross the clearing here to move from one forest to the other

Project costs

One objective of this research was to develop a method for obtaining aerial images that is low cost. In Table 3 an overview of the equipment cost is shown. The camera will consume the major part of the budget. Of course the camera can still be used as a normal camera.

Table 3: overview of the equipment cost

Kite Power sled large	80,-
Line (200 meters, 150 kg. breaking strength)	50,-
Line winder (homebuilt)	25,-
Remote control (incl. servo's)	160,-
Batteries	10,-
Camera canon s70	380,-
Extra memory card 1 gb	60,-
Extra battery	48,-
Gent led (Infra red remote control	17,-
Total expense	**830,-**

The major cost factor will be the software that is necessary to process the images to a final product.

Discussion

The objective of this research was to develop a cheap method to acquire high resolution aerial images. In this, the project has succeeded very well. The cost of the image acquisition system (kite, line, remote control and camera) were €830.- The obtained images could be used to create a very high resolution, georectified map and a digital elevation model. Kite or low aerial photography could improve the quality and accuracy of monitoring nature areas. High resolution imagery can be used to determine borders and transition zones between vegetation types with more accuracy then from ground level. The higher accuracy can be used to detect changes in the vegetation earlier then with conventional methods. To do this it is not always necessary to photograph an entire area. Depending on the size, photographing a large area could be time consuming. It is also possible to select several representative locations that can be photographed in a single shot. These locations can be fitted with fixed ground control markers so that follow up images can be easily processed. A single shot typically covers between the 0,5 and 3 hectare. When the ground control markers are already laid out a single shot can be taken within 15 minutes, including the time necessary to setup the kite gear. This means that taking an aerial photograph can be done while in the area for other field work. A database with very high resolution images over a longer time period can function as a reference database. It is an accurate representation of the real world without the bias of human interpretation.
The kite aerial images can also function as a powerful communication tool for policymakers or managers. The oblique (Birdseye-view) images give a quick overview over the landscape without becoming abstract.

However there are a lot of things that could improve:

Platform

The kite as a platform has several advantages and disadvantages. A kite is cheap, easy to operate and it requires no maintenance. It can be packed in a backpack and it causes no disturbance in the area while operating. On the other hand, a kite is not a very stable platform. Therefore the shutter speed needs to be high to minimize the amount of blurred images. Further it has proven to be quite hard to fly the kite in a fixed pattern although more experience in kite flying can overcome this problem. The wind direction sometimes makes is impossible to fly over the target area. Also manoeuvring around trees with the kite was difficult sometimes. The camera weight should be kept to a minimum to be able to use light winds. Besides kites there are several other types of platforms that are frequently used for low aerial remote sensing. When wind conditions are calm (< 1 Bft) a balloon can be used. Either helium (Boike et al., 2003) or hot air (Marzolff et al., 1997) can be used to lift a camera. A tethered balloon can be maneuvered quite precise over an area when there are more lines attached to it. Unfortunately, helium is a quite expensive non-renewable gas. One liter of helium gas will generate 1 gram of lift. This means that quite a volume of helium is necessary to lift a camera. The volume of a hot air

balloon is even bigger; however gas to heat the air is better availably in remote places then helium.
Remote controlled airplanes and helicopters are also a very suitable platform for acquiring aerial images. However, these are expensive, often not suitable for use in the field (sand and dust sensitive) and require a high level of experience to fly.
Parallel to this research at ITC a similar project was done that was using a remote controlled powered paraglider. The remote controlled paraglider is suitable for fieldwork conditions, needs a low experience level to operate and has a range of 5 km. The machine costs around € 12.000,-

GIS Software

The major cost factor for these projects is the software. There are however several software developers working on open source or freeware packages that can do the same thing (Grass GIS 6.0.2). The GIS package ILWIS, which was developed by ITC is expected to become open source in the summer of 2007.
There is also open source photo mosaic software. An example is HUGIN panorama tools. Although the software is not meant for photogrammetic purposes it is an excellent program to stitch aerial images.

Camera calibration

This step is very important for obtaining high accuracy. Unfortunately, camera calibration is a world on its own and there are a lot of different and confusing methods. The automated camera calibration procedure that Photomodeler offered was a very easy method to get the lens distortion parameters. However it was difficult to find out what the different parameters meant and how they had to be applied for use in Erdas photogrammetic suite.
Photomodeler 5 is quite expensive software. There are however less user-friendly, but cheap (or free) alternatives. Most of these come from robotics. When a robot is equipped with 'eyes', they use cameras. Those cameras also suffer from lens distortion and as a result the robot off sighted. The roboticanist produced a whole range of different tricks to solve that problem. Some of them are can be incorporated for use in photogrammetry (Zhang, 1998).

Ground control markers

The markers that were used as ground control points suffered from strong overcastting from the sun, which caused an extra inaccuracy. This could have been prevented by using different material as marker. Preferably the ground control markers also should have an identification mark, so it is easier to identify which coordinates belongs to which marker. In this research an expensive GPS was used. It is also possible to measure coordinates relative instead of absolute (linked to a geographical coordinate system) with an optical theodolite, or total station.

Classification

The images were suitable for visual identification of plant species. *Molinia caerulea* patches were easily identified because at the time of the photo acquisition their dead leaves had a high contrast with the surroundings. The mapping of heather types proofed more difficult. The spectral signature of *Calluna vulgaris* and *Erica tetralix* was very similar. Although the final result of the procedure used in this project was very acceptable, it would be easier when the images were acquired in August or September, when the heather flowers. Acquiring images in the flowering period also could give information about the vitality of the heather.

Pixel-base classification is a powerful technique to derive 'thematic classes' from remote sensing data. However, it has limitations. When using high resolution imagery a single plant can consist of several pixels that may vary due to shade, height or internal variation. This results in a misclassification when for instance the shadow side of a deciduous tree is classified as coniferous. There is a new technique called image segmentation that could solve some of the problems of pixel based image analysis. This method is becoming more and more important in remote sensing due to the increasing spatial resolution (Meinel et al., 2004)

Digital elevation map

The elevation maps showed very high detail. Even small depressions in the landscape were revealed. The images that were used gave a very good result. The other images also had a lot of overlap (>60%) but were for an unknown reason not suitable for use. More research is needed to improve the generation of digital elevation models with consumer digital cameras.

Multispectral remote sensing.

A digital camera with a ccd chip is capable of detecting infrared light. In appendix 7 there is an example of how to modify a digital camera for infrared photography. Vegetation has a high reflectance in the near infrared spectrum and this can be used for instance for a better classification of different plants species. The infra red band in combination with the red band can be used to calculate the ndvi to derive information about the quality of the vegetation. Gerard et al. (1997) used infrared light to measure plant growth and nitrogen status of pearl millet with kite aerial images.

In appendix 8 an effort is made to measure the spectral sensitivity of the Canon s70. This can be used to calculate the amount of reflected energy of a certain surface in watt/m^2. In temporal research this can improve the comparison between different dates because it can be used to compensate for different lighting conditions on different days. In theory, it would be possible to use a digital camera as a spectrometer. A spectrometer records, in very small wavelength bands, the reflection of a given surface. This can be used to create a spectral signature that surface. The spectral signature can be used in the classification process but also yields information about the nutrient content and amount of photosynthesis in vegetation.

By placing a grating in front of the lens the light entering the camera is spread out with respect to its wave length. By measuring the intensity of the spread-out light the spectral characteristics can be determined.

References.

Aber, J. S. 2002 Unmanned small format aerial photography from kites for acquiring large scale, high resolution multiview-angel imagery. Pecora 15/ land satellite information IV/isprs Commision I/FIEOS 2002 Conference Proceedings.

Aber, J.S. Aber, S.W. Pavri, F. Volkova, E. Penner, R. 2006 Small-format aerial photography for assessing change in wetland vegetation, Cheyenne Bottoms, Kansas. Transaction of the Kansas Acedemy of Science. 109, p.47-57

Aber, J.S Aaviksoo, K. Karofeld, E. 2003 Kite aerial photography – tool for microstructural investigations of mire ecosystems. Presented at XVI INQUA Congress

Baker, A. Fitzpatrick, B. Koehne, B. 2004 High resolution low altitude aerial photography for recording temporal changes in dynamic surficial environments. Regolith. pp. 21-25.

Boike, J. Yoshikawa, K. 2003 Mapping of Periglacial Geomorphology using kite / balloon aerial photography. Permafrost periglac. Process. 14: 81-85

Buerkert, A. Mahler, F. Marschner, H. 1996 Soil productivity management and plant growth in the Sahel: potential of an aerial monitoring technique. Plant and Soil 180: 29-38

Chandler, J.H. Fryer, J.G. Jack, A. 2005 Metric capabilities of low-cost digital cameras for close range surface measurment. Photogrammetic Record, 20: 12-26

Fairman, J. 1887 apparatus for Aerial Photography, Patentnumber 367610, United States Patent Office.

Gerard, B. Buerkert, A. Hiernaux, P. Marschner, H. 1997 Non-destructive measurements of plant growth and nitrogen status of pearl millet with low aerial photography. Soil Science Plant Nutrition's. 43: 993-998.

Hennemann, Nagelhout; 2002 Wind Erosion Mapping and Monitoring in the Central Rift Valley of Kenya Using Small-Format Aerial Photography (SFAP). 12th ISCO Conference Beijing

Marzolff, I. J.B. Ries. 1997. 35-mm photography taken from a hot-air blimp: Monitoring processes of land degradation in northern Spain. The first North American symposium on small format aerial photography, p. 91-101. Edited by Bauer et al., American Society for Photogrammetry and Remote Sensing.

Meinel, G. Neubert, M. A comparison of segmentation programs for high resolution remote sensing data. Leibniz institute of Ecological and regional development (IOER). http://www.isprs.org/istanbul2004/comm4/papers/506.pdf

Moore, T., Hill, C. J. and Napier, M. E. 2002. "Rapid Mapping with Post-Processed Data from Garmin Handheld Receivers." ION GPS 2002, 24-27 September, Portland, Oregon. 1414-1422.

Jia, L. Buerkert, A. Chen, X. Roemheld, V. Zhang, F. 2004 Low-altitude aerial photography for optimum N fertilization of winter wheat on the North China Plain. Field Crops Research. 89: 389-395

Macdonald w. 2002 Colour characterisation of a high resolution digital camera, Icolour & imaging institute, university of Derby, UK. Presented at the Colours in Graphics, Imaging and Vision (CGIV) conference, Poitiers.

Stow ,D Hope, A. Richardson, D. Chen, D. Garrisson, C. Service, D. 2000 Potential of colour-infrared digital camera imagery for inventory and mapping of alien plant invasions in South African shrublands. International journal of Remote Sensing, 21: 2965–2970

Thamm, H. The low cost drone, a new tool for the very high resolution remote sensing. Remote sensing research group, Institute for Geography, university of Bonn, Germany.http://www.rsrg.unibonn.de/Projekte/hape_dronen_Webpage/HP_Drone_00_start.html

Zhang, Z. 1998 A Flexible New Technique for Camera Calibration. Microsoft research.. http://research.microsoft.com/~zhang

Websites (1-1-2007) :
www.lifepixel.com

www.satimagingcorp.com/pricing.html

http://www.lvnl-ohd.nl : air traffic control Netherlands

http://grass.itc.it/index.php

http://www.itc.nl/ilwis/

http://hugin.sourceforge.net/

Appendix

Appendix 1: Air traffic control

OPS Helpdesk [OPS_Helpdesk@lvnl.nl]
Beste meneer Slot,
Ik heb hier wat navraag gedaan en zolang u buiten een straal van 5km rondom een vliegveld wilt vliegeren, volstaat dit inderdaad om dit middels een NOTAM te regelen. De regelgeving voor NOTAM uitgifte is dat dit 5 werkdagen van te voren moet worden gedaan. Dit kunt u het beste via ons laten regelen, dan zullen wij dit coordineren tussen de militairen en de burgerluchtvaartinstanties. De NOTAM aanvraag mag zowel telefonisch als via e-mail gedaan worden. Voor informatie over de ligging van diverse vliegvelden kunt u terecht op onze website (zie Handtekening).

Met vriendelijke groet,

Gert Muller
Operationele Helpdesk
Luchtverkeersleiding Nederland
Tel: +31-(0)20-4062201
Fax: +31-(0)20-4063672
E-mail: ops_helpdesk@lvnl.nl
Internet: http://www.lvnl-ohd.nl

Appendix 2: Camera Calibration Photomodeler 5 Status Report Tree

Information from most recent processing	Quality
FocalLength Value: 5.965779 mm Deviation: Focal: 0.004 mm Xp - principal point x Value: 3.539505 mm Deviation: Xp: 0.008 mm Yp - principal point y Value: 2.663596 mm Deviation: Yp: 0.007 mm Fw - format width Value: 7.188917 mm Deviation: Fw: 0.004 mm Fh - format height Value: 5.410200 mm K1 - radial distortion 1 Value: 7.110e-003 Deviation: K1: 4.4e-005 K2 - radial distortion 2 Value: -5.360e-004 Deviation: K2: 3.2e-006 K3 - radial distortion 3 Value: 2.122e-005 P1 - decentering distortion 1 Value: -3.080e-004 Deviation: P1: 4.3e-005 P2 - decentering distortion 2 Value: -6.903e-005 Deviation: P2: 4.1e-005	Photographs Total Number: 8 OK Photos: 8 Number Oriented: 8 Cameras Camera1: canon s70 Calibration: yes Number of photos using camera: 8 Point Marking Residuals Overall RMS: 0.318 pixels Maximum: 3.198 pixels Point 100 on Photo 1 Minimum: 0.183 pixels Point 10 on Photo 8 Maximum RMS: 1.480 pixels Point 100 Minimum RMS: 0.098 pixels Point 54 Point Precisions Overall RMS Vector Length: 0.000283 m Maximum Vector Length: 0.000449 m Point 100 Minimum Vector Length: 0.000219 m Point 48 Maximum X: 0.00029 m Maximum Y: 0.000286 m Maximum Z: 0.00022 m Minimum X: 8.73e-005 m Minimum Y: 9.03e-005 m Minimum Z: 0.000155 m

Appendix 3: Ground control points

Name point	x	y	height	x,y accuracy	height accuracy
B10	229624548	476249405	16.700	0,03	0,04
B11	229742705	476277070	18.712	0,03	0,04
B12	229858685	476401164	21.054	0,03	0,05
B13	229754465	476554045	17.500	0,02	0,04
B14	229789654	476647369	18.572	0,02	0,04
B15	229895855	476620079	22.052	0,03	0,05
B16	230026861	476536638	22.796	0,02	0,04
B17	230227247	476493435	18.969	0,02	0,04
B18	230353777	476342190	17.006	0,02	0,04
B19	230341946	476120348	19.233	0,04	0,07
B20	230335620	476125126	19.255	0,03	0,05
B21	230304038	476123511	19.460	0,02	0,04
B22	230164532	475984819	17.782	0,02	0,04
B23	230156623	475887945	17.787	0,02	0,03
B24	230012944	475895104	17.536	0,03	0,05
WMO0	230551526	476214985	16.901	0,02	0,04
WMO16	230559879	476213301	17.183	0,02	0,04
WMO17	230418252	476173458	18.552	0,02	0,04
WMO18	230401409	476141523	19.021	0,02	0,04
WMO19	230378767	476211591	18.463	0,02	0,04
WMO20	230341315	476252476	18.144	0,02	0,04
WMO21	230303251	476343049	18.016	0,02	0,04
WMÒ22	230249854	476188489	19.853	0,02	0,05
wMO233	230336434	476164691	19.339	0,04	0,04
WMO244	230359700	476153392	19.465	0,02	0,03
WMO23	230357648	476130018	18.855	0,02	0,03
WMO24	230506107	476215517	16.909	0,02	0,04
WMO25	230564465	476363082	16.359	0,02	0,03
WMO26	230649997	476261460	16.100	0,02	0,03
WMO27	230621747	476075252	18.731	0,02	0,03
WMO28	230711035	476098074	17.300	0,02	0,03
WMO29	230731066	476240524	16.262	0,02	0,03
C1	230609941	476377090	17.236	0,03	0,07
C2	230743437	476363070	16.844	0,02	0,05
C3	230701143	476434900	16.965	0,03	0,05
C4	230447169	476825448	17.088	0,02	0,04
C5	230305155	476776400	16.378	0,03	0,05

Appendix 4: Exterior orientation parameters

The	exterior	orientation	parameters			
imageID	Xs	Ys	Zs	OMEGA	PHI	KAPPA
1	230284	476362	176.3282	0.8465	5.3231	-10.2585
16	230393	476365.6	171.9107	191.0795	171.1069	-192.4
4	230251.9	476303.3	171.5663	1.8382	6.2989	-21.9667
3	230260.9	476310.8	192.8752	1.5271	17.0434	-6.8933
15	230405.6	476258.9	151.5468	6.99	7.9642	72.6271
5	230249.9	476237.8	163.4556	1.5237	7.5856	-8.8366
6	230243.1	476207.7	165.4026	6.3272	15.3427	-26.9246
12	230359.8	476182.1	149.6756	-350.335	351.5423	-454.343
13	230371.3	476199.3	175.4105	-8.1456	19.0836	90.2786
14	230376.7	476218.6	163.8314	-7.3419	4.212	88.1486
2	230401	476232	145.8233	-7.4739	5.3699	91.2642
8	230259.6	476134.6	158.6009	-1.902	21.5288	85.3861
9	230277.7	476134.1	157.9011	-378.235	6.4342	439.7735
10	230327.8	476163	162.3297	-2.5292	2.597	71.8122
11	230330	476165.1	160.8997	3.5645	5.2037	66.488
7	230199.2	476086.2	206.5692	8.5198	6.5206	-7.6741

Appendix 5: Mayority filter

To reduce the amount of misclassified pixels a majority filter is used. A majority filter looks in a raster e.g. 3x3 or 5x5 which class occurs the most frequently and assigns that class to the whole matrix.

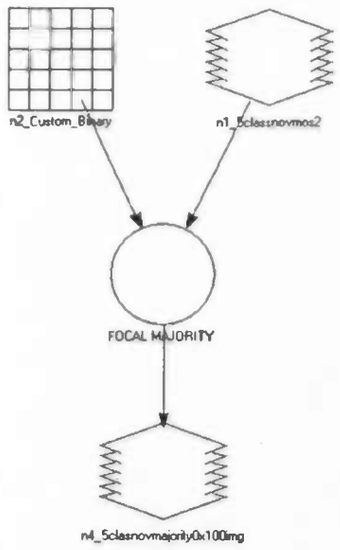

Appendix 6: DEM accuracy report

Global DEM info	General Mass Point Quality:	number of 3D Reference Points Used: 23
Cell Width: 0.2000 meters	Excellent % (1-0.85): 43.3533 %	Minimum, Maximum Error: -1.2160, 0.4774
Minimum Mass Point Elevation: 16.5254	Good % (0.85-0.70): 35.1864 %	Mean Error: -0.0436
Maximum Mass Point Elevation: 32.8606	Fair % (0.70-0.5): 0.0000 %	Mean Absolute Error: 10.6520
Mean Mass Point Elevation: 19.6972	Isolated %: 0.0000 %	Root Mean Square Error (RMSE): 0.4537
	Suspicious %: 21.4602 %	Absolute Linear Error 90 (LE90): 0.6920
		NIMA Absolute Linear Error 90: +/- 0.0000

Appendix 7: Modifying digital camera for Near Infrared (NIR)

Digital cameras use a ccd- chip (charged-coupled device) to record light. In contrast to the human eye, ccd-chips are sensitive to near infrared light. Visible light has a wavelength range between 350 and 720 nm. where as ccd-chips are sensitive for near infrared wavelengths between 350 and 1000 nm. This extended sensitivity in wavelength range would result in a dominance of red in a normal photograph. Therefore manufactures of digital cameras install an infrared cut-off filter in front of the ccd- to prevent IR-light reaching the chip.

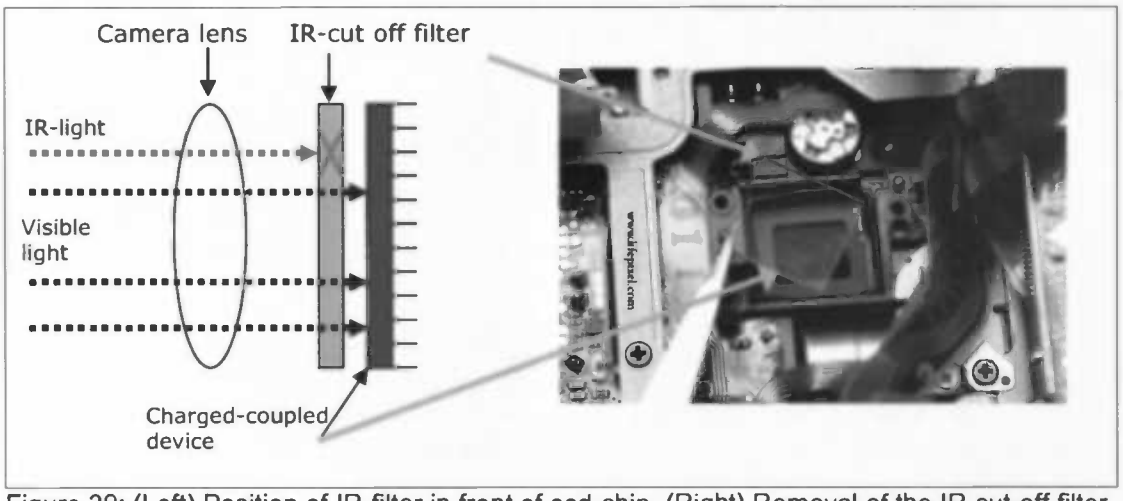

Figure 39: (Left) Position of IR-filter in front of ccd-chip. (Right) Removal of the IR cut-off filter.

To be able to record infrared light with a normal digital camera, the IR cut-off filter is replaced by a normal piece of glass. This piece of glass needs to have more or less the same characteristics (breaking-index) as the IR cut-off filter has, otherwise the camera characteristics might change. To collect only infrared light, a filter that blocks visible light has to be installed. By using two digital cameras that fire simultaneously it is possible to record 4 wavelength bands. One camera registers the normal visible colours, bleu, green and red, while the other registers infrared.

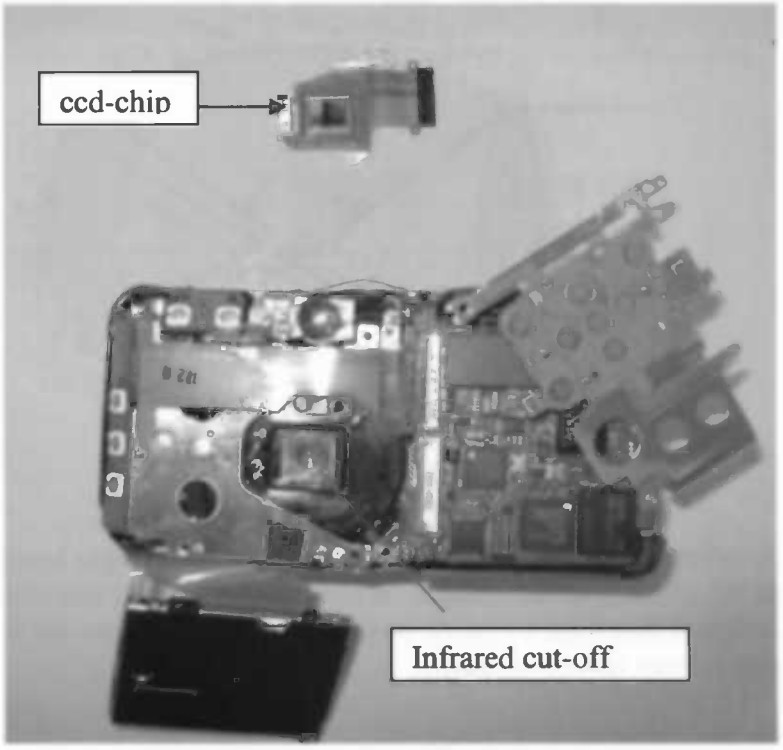

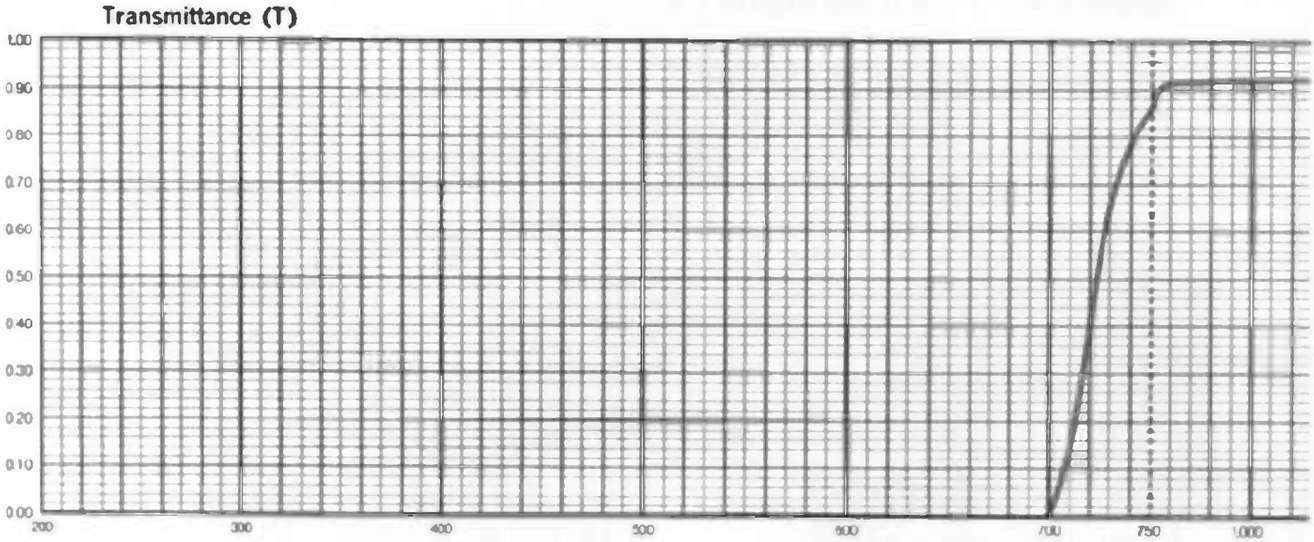

Source: http://www.hoyaoptics.com/pdf/R72.pdf . The transmittance of infrared light through a Hoya R72 filter. Because these filters don't have sharp cut-offs the 50% transmittance is used to describe the filter characteristics. The R72 filter transmits wavelengths that are greater then 720 nm.

To be able to compare images taken on different days, daylight variations have to be taken in account. The camera used in this research has a custom white balance function which measures and adjusts the white balance to the present light conditions. By measuring the light reflected from a standard grey sheet of paper the images are adjusted for different light conditions.

- focus/chromatic aberration

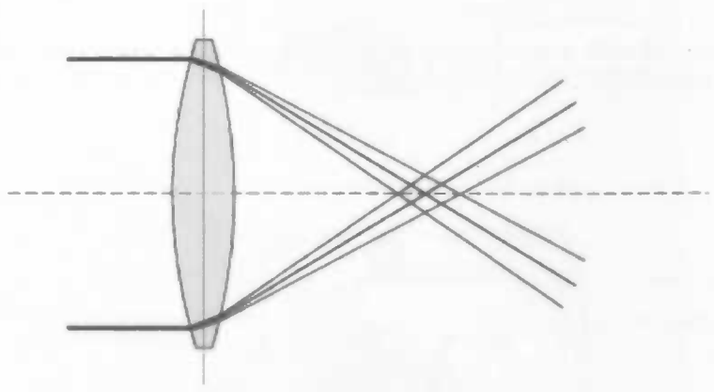

Another aspect has to be taken in account. Wide angle lenses tend to have a distortion at the corners of the images. When using a normal unmodified camera the camera is adjusted that light of every wavelength is in focus on the ccd. For near infrared light this is even more a problem.

Infrared test photos

The images on the left are taken with an unmodified digital camera. The images on the right are taken with a modified digital camera. The right images taken with the modified digital camera are near infrared images. The wavelength of the recorded light ranges from 720 nm. till 1000 nm.

Figure 39: the left images are normal digital photos, the images on the left are taken with a infrared camera.

Appendix 8: Spectral response curve

A experimental setup was build in cooperation with the University of Twente to determine the spectral sensitivity of the ccd chip of the Canon s70. This was done with a monochromator. A monochromator is a device that, with the use of gratings, allows only light of a certain wavelength to pass. By photographing the exit of the monochromator in camera RAW format, the unprocessed light intensities are recorded for each different wavelength.

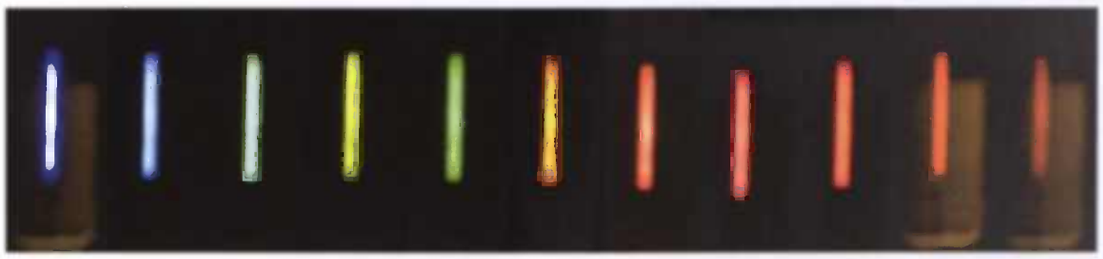

Figure 38: Photos of the output of the monochromator with their wavelength (Nm). The photos cover the whole visible spectrum with intervals of 25 Nm.

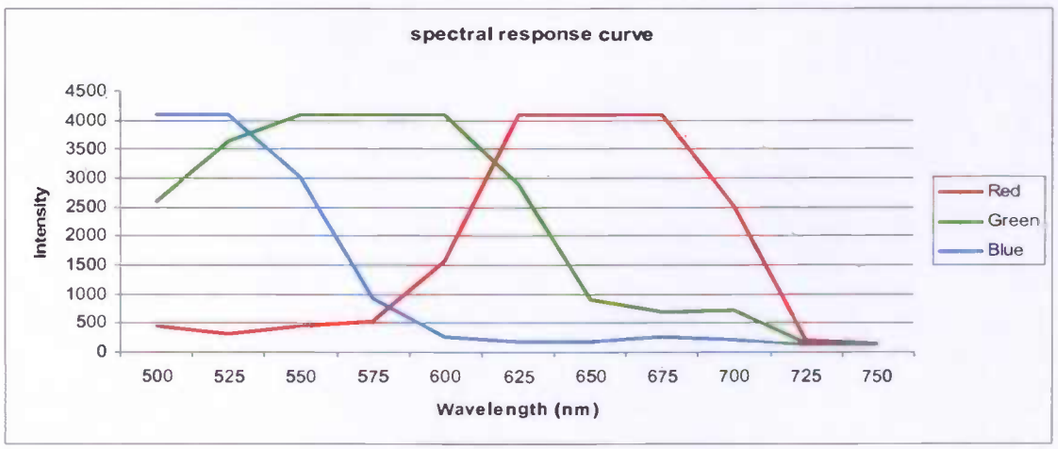

Figure 39:. In this graph the sensitivity off the ccd-chip for each channel is shown based on the images in **Figure 38**. Unfortunately the top of the curves are missing as a result of a wrong exposure time.

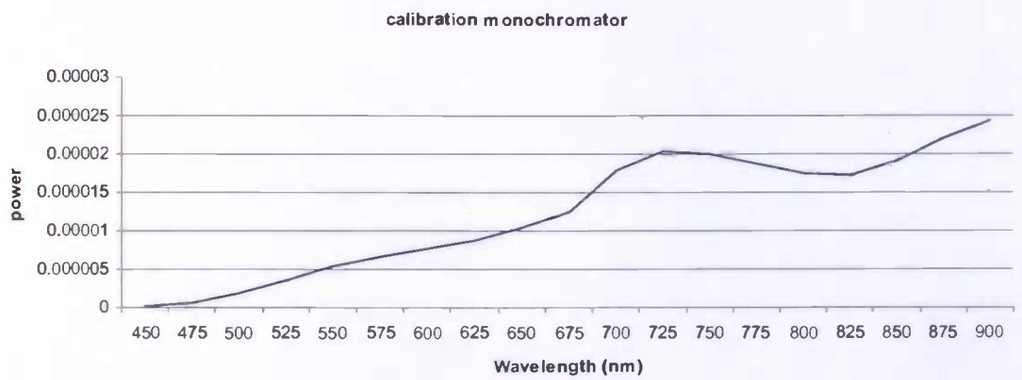

Figure 6: The output of the monochromator is measured with a spectrometer. This gives the amount of energy at the output of the monochromator for any given wavelength. With this data it is possible to calculate the sensitivity of the ccd sensor in W/m2 for certain camera setting.